AD-A164 793 ELECTRICAL MEASUREMENTS ON ALPHA-QUARTZ CRYSTALS(U) 1/1
HENRY KRUMB SCHOOL OF MINES NEW YORK A S NOWICK DEC 85
RADC-TR-85-174 F19628-82-K-0013

UNCLASSIFIED F/G 20/2 NL

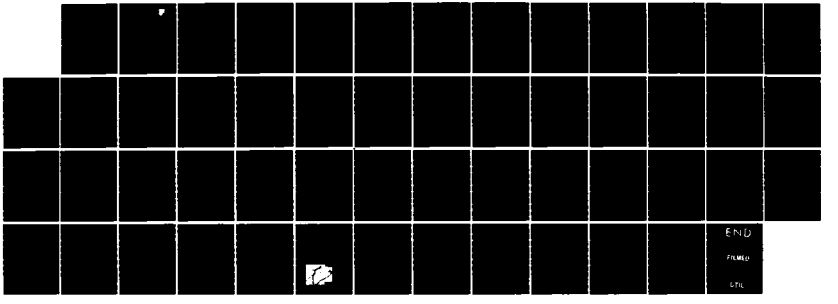

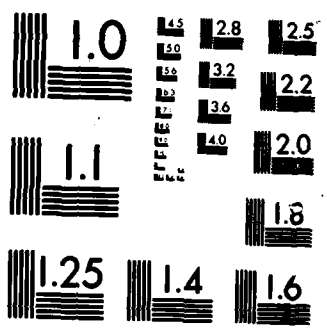

(12)

RADC-TR-85-174
Final Technical Report
December 1985

ELECTRICAL MEASUREMENTS ON α -QUARTZ CRYSTALS

Columbia University

A. S. Nowick

APPROVED FOR PUBLIC RELEASE; DISTRIBUTION UNLIMITED

ROME AIR DEVELOPMENT CENTER
Air Force Systems Command
Griffiss Air Force Base, NY 13441-5700

This report has been reviewed by the RADC Public Affairs Office (PA) and is releasable to the National Technical Information Service (NTIS). At NTIS it will be releasable to the general public, including foreign nations.

RADC-TR-85-174 has been reviewed and is approved for publication.

APPROVED: Herbert G. Lipson

HERBERT G. LIPSON
Project Engineer

APPROVED: Harold Roth

HAROLD ROTH, Director
Solid State Sciences Division

FOR THE COMMANDER: John A. Ritz

JOHN A. RITZ
Plans Office

If your address has changed or if you wish to be removed from the RADC mailing list, or if the addressee is no longer employed by your organization, please notify RADC (ESE) Hanscom AFB MA 01731. This will assist us in maintaining a current mailing list.

Do not return copies of this report unless contractual obligations or notices on a specific document requires that it be returned.

UNCLASSIFIED

SECURITY CLASSIFICATION OF THIS PAGE

AD-A164793

REPORT DOCUMENTATION PAGE

1a REPORT SECURITY CLASSIFICATION UNCLASSIFIED	1b RESTRICTIVE MARKINGS N/A
2a SECURITY CLASSIFICATION AUTHORITY N/A	3 DISTRIBUTION / AVAILABILITY OF REPORT Approved for public release; distribution unlimited
2b DECLASSIFICATION / DOWNGRADING SCHEDULE N/A	
4 PERFORMING ORGANIZATION REPORT NUMBER(S) N/A	5 MONITORING ORGANIZATION REPORT NUMBER(S) RADC-TR-85-174
6a NAME OF PERFORMING ORGANIZATION Columbia University 6b OFFICE SYMBOL (If applicable)	7a NAME OF MONITORING ORGANIZATION Rome Air Development Center (ESE)
6c ADDRESS (City, State, and ZIP Code) Henry Krumb School of Mines New York NY 10027	7b ADDRESS (City, State, and ZIP Code) Hanscom AFB MA 01731
8a NAME OF FUNDING / SPONSORING ORGANIZATION Rome Air Development Center 8b OFFICE SYMBOL (If applicable) ESE	9 PROCUREMENT INSTRUMENT IDENTIFICATION NUMBER F19628-82-K-0013
8c ADDRESS (City, State, and ZIP Code) Hanscom AFB MA 01731	10 SOURCE OF FUNDING NUMBERS PROGRAM ELEMENT NO: 61102F; PROJECT NO: 2305; TASK NO: J1; WORK UNIT ACCESSION NO: 725

11 TITLE (Include Security Classification)

ELECTRICAL MEASUREMENTS ON α - QUARTZ CRYSTALS

12 PERSONAL AUTHOR(S)

A.S. Nowick

13a TYPE OF REPORT	13b TIME COVERED	14 DATE OF REPORT (Year, Month, Day)	15 PAGE COUNT
Final	FROM Nov 81 TO Dec 84	December 1985	54

16 SUPPLEMENTARY NOTATION

N/A

17 COSATI CODES		
FIELD	GROUP	SUB-GROUP
20	01	

18 SUBJECT TERMS (Continue on reverse if necessary and identify by block number)

Quartz — Electrical properties
Defect Structure of Solids

19 ABSTRACT (Continue on reverse if necessary and identify by block number)

This study was aimed at achieving a better understanding of the defects in α-quartz crystals that affect their frequency stability. The principal techniques used were electrical conductivity and dielectric loss measurements, both of which are largely controlled by alkalis present to compensate for substitutional $Al^{(3+)}$. In order to deal with just one alkali species at a time, samples studied were swept with either Li^+ or Na^+.

The results involve considerable information about Al-Na and Al-Li bound pairs in the crystal, about alkalis freed from these pairs that give rise to the conductivity, and about the defects (which include electrons and holes) produced by X-ray irradiation of these crystals. The Al-Na pairs can exist in two configurations (α and β) with the Na on opposite sides of the AlO_4 tetrahedron, off the C_2 symmetry axis. In Al-Li, however, the Li^+ sits on the C_2 axis. The alkalis freed at high temperature give rise to the conductivity and involve a higher activation energy for Li^+ and for Na^+. Finally, upon irradiation, liberated alkalis form new centers which produce a striking low-temperature dielectric loss peak. The use of (over)

20 DISTRIBUTION / AVAILABILITY OF ABSTRACT	21 ABSTRACT SECURITY CLASSIFICATION
☐ UNCLASSIFIED/UNLIMITED ☒ SAME AS RPT ☐ OTIC USERS	UNCLASSIFIED
22a NAME OF RESPONSIBLE INDIVIDUAL Herbert G. Linson	22b TELEPHONE (Include Area Code) (617) 861-3297
	22c OFFICE SYMBOL RADC (ESE)

DD FORM 1473, 84 MAR — 83 APR edition may be used until exhausted. All other editions are obsolete

SECURITY CLASSIFICATION OF THIS PAGE

UNCLASSIFIED

Block 19. Abstract (Cont'd)

computer simulation calculations has also been shown to be a helpful adjunct to the electrical measurements.

SUMMARY

This study was aimed at achieving a better understanding of the defects in α-quartz crystals that affect their frequency stability. The principal techniques used were electrical conductivity and dielectric loss measurements, both of which are largely controlled by alkalis present to compensate for substitutional Al^{3+}. In order to deal with just one alkali species at a time, samples studied were swept with either Li^+ or Na^+.

The results involve considerable information about Al-Na and Al-Li bound pairs in the crystal, about alkalis freed from these pairs that give rise to the conductivity, and about the defects (which include electrons and holes) produced by X-ray irradiation of these crystals. The Al-Na pairs can exist in two configurations (α and β) with the Na on opposite sides of the AlO_4 tetrahedron, off the C_2 symmetry axis. In Al-Li, however, the Li^+ sits on the C_2 axis. The alkalis freed at high temperature give rise to the conductivity and involve a higher activation energy for Li^+ than for Na^+. Finally, upon irradiation, liberated alkalis form new centers which produce a striking low-temperature dielectric loss peak. The use of computer simulation calculations has also been shown to be a helpful adjunct to the electrical measurements.

I. INTRODUCTION

In attempting to understand the various point defects in α-quartz crystals which affect their frequency stability, we have emphasized the use of two electrical techniques: electrical conductivity measurement and dielectric relaxation. The most important impurity appears to be Al^{3+} substituting for Si^{4+}. Because of the difference in ionic charge, each Al^{3+} is compensated by the presence of either an interstitial alkali ion, Na^+ or Li^+, or a proton H^+ which together with an oxygen ion forms an OH^- bond. In order to avoid, as much as possible, the complexity of having more than one of these three compensating ions present in the crystal, this work has focused on studying samples that have been electrodiffused, or "swept", with either Na^+, Li^+, or H^+. In addition, most of the work has been done on samples that had been characterized by other techniques such as infrared (IR) measurements (which detect various OH^- configurations), internal friction (which detects Al-Na and other defects) and electron spin resonance (ESR) (which detects Al-hole centers after irradiation). These other techniques have been utilized at the Rome Air Development Center (Hanscom AFB) and at Oklahoma State University. Accordingly, many of the samples studied at Columbia were interchanged with these two groups in order to achieve the most complete characterization possible. With such collaborations, we have been able to show that the electrical techniques yield considerable additional information that compliments the other techniques.

II. REVIEW OF RESULTS

The work under this contract has resulted in several papers which are listed on page 8 of this report. The present review will merely summarize the principal results and conclusions, and referring to the specific papers for details. The work naturally divides itself up into that on dielectric

relaxation versus that on conductivity, and also of work on unirradiated crystals versus that on irradiated crystals. The subsections of this report are labeled accordingly.

A. Dielectric Relaxation of Unirradiated Crystals

(Papers 1, 2 and 5)

A detailed study was made of the two loss peaks that are caused by the Al-Na defect. These peaks, known as the α and β peaks, occur at 30 K and 75.4 K, respectively, for a frequency of 1 kHz. They are very sharp peaks (almost perfect Debye relaxations) and are shown to correspond to two inequivalent α and β configurations whereby the Na^+ sits on opposite sides of the AlO_4 distorted tetrahedron.

Precise values of the activation energies (50 and 127 meV, respectively) and the frequency factors for the two peaks were obtained. In addition, it was conclusively demonstrated (see Paper 5) that the α and β configurations are not in equilibrium below room temperature, showing that a high activation energy is involved for the Na^+ to pass across the tetrahedron from α to β or from β to α .

The two peaks were calibrated in terms of the absolute concentrations of Al-Na in both the α and β configurations, so that henceforth these peaks can be used to quantitatively determine these defect concentrations.

In the case of Li^+ swept samples, no peaks were found (to a good precision). It is thus possible to conclude that for Al-Li, the Li^+ ion sits on the 2-fold symmetry axis of the AlO_4 tetrahedron, unlike the Al-Na case.

Preliminary relaxation experiments were carried out on an amethyst crystal (containing Fe^{3+}). A new relaxation peak in this crystal was found near 100K (for 1 kHz). It is close to a Debye peak and has an activation energy of 0.19 eV. It is reasonable to associate this peak with the presence of iron, but to determine just how the alkali is related requires further study.

B. Conductivity of Unirradiated Crystals

(Papers 1 and 3)

It has been known for some time that electrical conduction in unirradiated quartz is ionic in nature and takes place by migration of alkali ions under the applied electric field.

A whole series of measurements were made on various crystals: natural and cultured; high, medium and low aluminum; Li-swept and Na-swept. It was shown that the activation energy is somewhat higher for Li-swept than for Na-swept samples (by about 0.06eV) showing that the association energy E_A of the Al-Li pair is higher than that of the Al-Na pair. Very low ($\sim$ 2 orders of magnitude lower) conductivities were found for H-swept and ultra-high purity (General Electric, UK) crystals. Yet both of these latter crystals showed the activation energy (1.42 eV) characteristic of Li conduction, indicating that conduction was still taking place by migration of residual Li^+.

The failure of the conductivity to vary monotonically with the alkali content, as well as detailed analysis of the magnitude of the pre-exponentials of the conductivity, support a model (advanced by Jain and Nowick) in which some of the Al^{3+} present is compensated by defects other than M^+ or H^+ (possibly oxygen-ion vacancies). Only in terms of such a model can the conductivity be interpreted quantitatively.

C. Computer Simulation Calculations

Recently we have begun a joint program with Dr. C.R.A. Catlow of University College London (UK) to carry out computer simulated defect calculations for α-quartz crystals (with support from a NATO travel grant). These methods have previously been applied with great success to the study of various halides and oxides whose bonding is largely ionic. In the case of quartz, where bonding is

partially covalent, it has been necessary to introduce three-body, angle dependent, terms. Preliminary calculations have been carried out showing that:

a) the Li^+ in Al-Li sits on the 2-fold symmetry axis, while Na^+ in Al-Na is off the axis in two inequivalent positions (α and β) on opposite sides of the AlO_4 tetrahedron;

b) the $\alpha \rightarrow \beta$ and $\beta \rightarrow \alpha$ jumps for Al-Na involve a high activation energy ($\sim$ 1.4 eV);

c) the association energy for Al-Li is considerably higher than that for Al-Na, so that the net activation energy for conductivity of Na-swept samples is lower than that for Li-swept.

All of these results of the calculations agree very well with the experimental results quoted earlier.

D. Dielectric Relaxation of Irradiated Crystals

(Papers 1, 2 and 4)

Irradiation was carried out using X-rays from a tungsten target tube run at 40 kV and 20 mA. Doses were in the vicinity of 2×10^6 rads.

In Na swept samples, room temperature irradiation greatly lowers or eliminates the Al-Na peaks and replaces them with a very low temperature peak (near 9 K) which we will henceforth call the "irradiation peak". A similar irradiation peak is also observed in Li-swept samples but it does not occur at exactly the same temperature as in the Na-swept sample. Further, the irradiation peaks in a natural crystal (both Na and Li swept) occur at higher temperatures than do those in the cultured (Toyo) crystal studied. The annealing behavior of the irradiation peak is also different for Li-swept and Na-swept samples (see paper 2).

The irradiation peaks show considerable distortion from the usual behavior, on 1/T plots. Detailed study has shown that this is due to quantum effects, particularly below $\sim$ 6 K, such that the relaxation time no longer follows

Arrhenius behavior but instead goes as 1/T. The latter behavior is characteristic of quantum mechanical phonon-assisted tunneling.

It has been concluded that the irradiation peaks may be due to alkalis that are freed from Al-M defects and have captured electrons. On the other hand they may be due to Al-hole centers, but because of differences in the peak for different samples (Li vs. Na, natural vs. cultured) the peak would then have to be regarded as an Al-hole center perturbed by the presence of other defects. Further investigations now under way are aimed at resolving the question of the origin of the irradiation peak. In any case, the quantum behavior and the very low peak temperature suggests that the jumping entity is the electronic component (electron or hole) of the defect involved.

E. Conductivity of Irradiated Crystals

(Paper 3)

In one set of experiments samples were irradiated below room temperature (between 150 and 250 K) and conductivity measured in situ as a function of temperature immediately thereafter. The conductivity at these low temperatures is enhanced by the irradiation (relative to the unirradiated) by a factor as high as 10^{11}, a truly spectacular effect! The conductivity immediately following irradiation repeatedly shows a unique activation energy of 0.29 ± 0.01 eV. As the temperature is raised the conductivity continues to anneal.

Irradiation above 200 K is expected to free alkalis which should then contribute to the enhanced conductivity. However, 150 K irradiation produces a higher conductivity than 210 K irradiation, although alkalis have been shown (in work at Oklahoma State) not to be freed at 150 K.

The remaining conductivity experiments were carried out by irradiating at room temperature and making measurements at higher temperatures. In this study, a surprising cross-over effect was found, in which the conductivity anneals to

values below that of the unirradiated sample and then (above $\sim$ 500 K) anneals upward.

The totality of evidence from both sets of conductivity experiments, both below and above room temperature, favors not alkalis but free holes (polarons) as carriers immediately after irradiation. The cross over is then due to the annealing out of the holes and the restoration of alkali-controlled conduction. The unique activation energy of 0.29 eV is then attributed to polaron hole migration. Evidence in the literature from photoelectron spectroscopy studies seems to support these ideas, but further work is still required to firmly establish the defect mechanism.

III. CONCLUSIONS

The study of electrical properties, specifically conductivity and dielectric loss, both before and after irradiation, has been shown to provide powerful techniques for evaluating the nature and properties of defects in α-quartz crystals. This is especially true when swept crystals are studied and when the electrical measurements are complimented by other techniques, e.g. IR, ESR and internal friction.

Our studies have produced detailed information about the structure and properties of Al-Na and Al-Li defects, and about the effects of irradiation in generating different defects involving electrons and holes. The use of computer simulation calculations has also been shown to be useful in understanding these defects.

Continued use of both the electrical measurements and computer simulation in conjunction with other experimental techniques promises to reveal considerably more information about defects in quartz and the manner in which they are altered by irradiation.

Papers Prepared Under This Contract

1. J. Toulouse, E.R. Green and A.S. Nowick, "Effect of Alkali Ions on Electrical Conductivity and Dielectric Loss of Quartz Crystals", Proc. 37th Ann. Symp. Freq. Control, USAERADCOM, p. 125 (1983).
2. J. Toulouse and A.S. Nowick, "Dielectric Loss in Li- and Na-swept α-Quartz and the Effect of Irradiation", in Defect Properties and Processing of High-Technology Nonmetallic Materials, ed. J.H. Crawford et al., North-Holland (1984), p. 149.
3. E.R. Green, J. Toulouse, J. Wacks and A.S. Nowick, "Effect of Irradiation and Annealing on the Electrical Conductivity of Quartz Crystals", in Proc. 38th Ann. Symp. on Freq. Control, IEEE, p. 32 (1984).
4. A.S. Nowick, "Some Techniques for the Study of Atomic Motions with Applications to Ceramic Materials", in Proc. 2nd Israel Materials Engineering Conference, ed. A. Grill and S.I. Rokhlin, p. 11, (1984).
5. J. Toulouse and A.S. Nowick, "Dielectric Loss of Quartz Crystals Electrodiffused with Either Na^+ or Li^+." J. Phys. Chem. Solids, in press.

The five above papers are appended to this report.

Presentations at Conferences

1. J. Toulouse, E.R. Green and A.S. Nowick, "Effect of Alkali Ions on Electrical Conductivity and Dielectric Loss of Quartz Crystals." At 37th Ann. Symposium on Frequency Control, Philadelphia, June 1983.
2. J. Toulouse and A.S. Nowick, "Dielectric Loss in Li- and Na-Swept α-Quartz and the Effect of Irradiation" Materials Research Society, Boston, November 1983.
3. E.R. Green, J. Toulouse, J. Wacks and A.S. Nowick, "Effect of Irradiation and Annealing on the Electrical Conductivity of Quartz Crystals." At 38th Ann. Symp. on Frequency Control, Philadelphia, June 1984.
4. A.S. Nowick, "Some Techniques for the Study of Atomic Motions with Applications to Ceramic Materials". At 2nd Israel Conf. on Materials Engineering, Beer Sheva, Israel, February 1984.
5. J. Toulouse and A.S. Nowick, "Effect of Irradiation on the Annealing of the Electrical Conductivity of Quartz Crystals." At Int. Conf. on Defects in Insulating Crystals, Salt Lake City, Utah, August 1984.
6. A.S. Nowick and J. Toulouse, "Low Temperature Dielectric Relaxation in X-Irradiated Alpha Quartz." American Physical Society, Baltimore, Md., March 1985.

DIELECTRIC LOSS OF QUARTZ CRYSTALS ELECTRODIFFUSED WITH EITHER Na^+ OR Li^+

J. TOULOUSE† and A. S. NOWICK
Henry Krumb School of Mines, Columbia University, New York, NY 10027, U.S.A.

(*Received* 11 *April* 1985; *accepted* 9 *May* 1985)

Abstract—Dielectric relaxation techniques were used in order to better understand the behavior of defects that affect the frequency stability of α-quartz crystals. Crystals were studied that have been swept (electrodiffused) either with Na^+ or with Li^+. The Na-swept samples showed two well-known loss peaks (called α and β) due to the Al–Na pair, corresponding to the Na^+ ion, respectively, in nn and nnn interstitial sites about a substitutional Al^{3+} ion. Precise activation energies and preexponentials were obtained by comparison with analogous anelastic loss peaks. It was also found that the α:β equilibrium is frozen-in below 300 K and can be varied, by heat treatment. Values of the components of the dipole moment of the α and β pairs were determined, and absolute calibrations obtained for the two peaks. In the case of the Li-swept samples, however, there were no peaks present, from which it was concluded that for the Al–Li pair, the Li^+ ion sits on the twofold symmetry axis of the AlO_4 tetrahedron.

Keywords: dielectric relaxation, α-quartz, electrodiffusion, dielectric loss, point defects

1. INTRODUCTION

Crystalline quartz has become the foremost material in ultrasonic devices and precision frequency standards. Most high-stability oscillators use quartz crystals as a frequency standard and often there are very severe demands made on their frequency stability. As a result of such applications there has been a renewed interest in fundamental studies of quartz, and in particular, in the nature and behavior of point defects that are present.

Perhaps the most important defects in quartz involve an Al^{3+} impurity substituting for Si^{4+}. Since the Al has a lower valence than Si, an additional defect is required for charge compensation. This is usually provided by an interstitial alkali ion (mainly Na^+ and Li^+) or by H^+. The alkali becomes bound to the Al by coulombic attraction to form an Al–M^+ pair, while H^+ forms an OH bond near the Al. The presence of the Al–OH defect is detectable by infrared measurements [1–3]. The study of alkalis in quartz is particularly important, since frequency drifts under irradiation have been shown to be related to their presence [3–6].

The pioneering work of Stevels and Volger [7] revealed a pair of dielectric loss peaks at low temperatures that could be attributed to the Al–Na defect. These peaks, appearing at 38 and 95 K for a frequency of 32 kHz, have been termed the α and β peaks, respectively. Detailed analyses of these peaks in terms of the general theory of relaxation phenomena [8] was given by Nowick and Stanley [9] and further measurements and analysis were reported by Park and Nowick [10]. A related pair of anelastic peaks has also been observed in AT cut resonators oscillating at 5 MHz [11, 12]. All of these results support a model in which a Na^+ ion resides about the AlO_4 tetrahedron in one of two inequivalent positions: α (nn position) and β (nnn position). Because the tetrahedron is distorted, its only symmetry is a twofold rotation axis (C_2), as shown in Fig. 1. Consequently, there exists on each tetrahedron two equivalent α and two β sites, and the relaxation processes involve reorientations among these configurations.

Stevels and Volger [7] also reported a loss peak at 60 K which they attributed to the Al–Li defect, and Fraser [11] reported an anelastic peak attributed to Li.

In all of this earlier work there was no control by the investigator of the type of alkali present in the crystal. A method called electrodiffusion or "sweeping" had been introduced [1, 4, 11], however, making possible the substitution of one alkali for another, by applying an electric field parallel to the c-axis of the crystal at an elevated temperature ($\sim$500°C). A salt containing the desired alkali is placed at the sample–anode interface prior to the electrolysis. This technique has recently been refined by Martin [12], and utilized in the present work to produce samples in which virtually all of the Al^{3+} is compensated either by Na^+ or by Li^+ (called "Na-swept" and "Li-swept" samples, respectively). In this way, the complexity of having both alkalis present at the same time can be avoided.

In this paper we report on a study, by dielectric relaxation measurements, of both Na-swept and Li-swept quartz crystals. The work on the Na-swept samples leads to a more detailed understanding of the Al–Na defect than had hitherto been achieved. The study of Li-swept samples was aimed at determining whether or not there are analogous loss peaks attributable to the Al–Li defect.

2. THEORY

Dielectric loss can arise from defects which have a lower point symmetry than that of the crystal in which

† Present address: Physics Department, Lehigh University, Bethlehem, PA 18015.

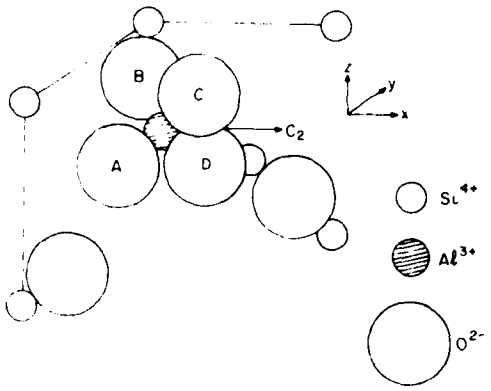

Fig. 1. Schematic diagram showing part of the unit cell of α-quartz containing an AlO_4 tetrahedron with Al^{3+} substituted for Si^{4+}. This distorted tetrahedron contains a single twofold symmetry axis (in the x direction), designated C_2.

they reside [8]. Such defects possess several crystallographically equivalent orientations, among which they may reorient preferentially in the presence of an electric field. If the electric field is sinusoidal with angular frequency ω, one or more peaks will usually occur in the dielectric loss, $\tan\delta$, which obey the well-known Debye equation:

$$\tan\delta \quad \frac{\delta\epsilon}{\epsilon_\infty}\frac{\omega\tau}{1+\omega^2\tau^2}, \tag{1}$$

where ϵ_∞ is the dielectric constant observed at high frequencies, $\delta\epsilon$ is called the relaxation of the dielectric constant and τ is the relaxation time given by

$$\tau^{-1} = \nu_0 \exp(-H/kT). \tag{2}$$

Here H is the enthalpy of activation, kT has its usual meaning, and ν_0 is the effective frequency factor, which includes a term containing the entropy of activation.

In α-quartz, which has trigonal symmetry, the highest site symmetry is that of the Si^{4+} ion. This site is monoclinic and involves a two-fold (C_2) axis which is taken along the x-axis. The Si^{4+} sits at the center of a distorted SiO_4 tetrahedron. When Al^{3+} is present, it substitutes for an Si^{4+} at the tetrahedron center as shown in Fig. 1. If the Al^{3+} is compensated by an interstitial alkali M^+ sitting nearby, this substitutional-interstitial pair forms a triclinic defect so long as the M^+ is not located on the C_2-axis. Such a defect has six equivalent orientations: two on each tetrahedron, and three differently oriented tetrahedra (each rotated through 120° from the other) in each unit cell. For the defect to move from one tetrahedron to another, however, requires migration of the Al^{3+} ion. The activation energy for such a process is anticipated to be far too high for such a jump to take place in the temperature range of the present experiments. Accordingly, relaxation occurs only by reorientation of the pair across the C_2 axis of each tetrahedron, a process that requires only an interstitial jump of the M^+ ion. The fact that the Al–Na pair is responsible for two separate relaxation peaks, which we here call the α and β peaks, inevitably means that the pair exists as two nonequivalent triclinic species (α and β) each of which can undergo reorientation under a field. Nowick and Stanley [9] have given expressions for the relaxation magnitudes in such a situation under the reasonable assumption that the fastest interstitial jump is that between the two α defect orientations on a given AlO_4 tetrahedron. This results in low-temperature relaxations whose magnitudes involve only the dipole moments of the α defects, and consequently the higher temperature (slower) relaxation involving only the β defect. They showed that the relaxation magnitudes for the lower temperature are given by

$$\delta\epsilon_{\parallel}^{\alpha} = N_\alpha \mu_3^{\alpha 2}/\epsilon_0 kT; \quad \delta\epsilon_{\perp}^{\alpha} = N_\alpha \mu_2^{\alpha 2}/2\epsilon_0 kT, \tag{3a}$$

and for the higher temperature, by

$$\delta\epsilon_{\parallel}^{\beta} = N_\beta \mu_3^{\beta 2}/\epsilon_0 kT; \quad \delta\epsilon_{\perp}^{\beta} = N_\beta \mu_2^{\beta 2}/2\epsilon_0 kT, \tag{3b}$$

where ϵ_0 is the permittivity of vacuum, $\delta\epsilon_{\parallel}$ and $\delta\epsilon_{\perp}$ are the relaxations for directions, respectively, parallel and perpendicular to the crystallographic c-axis, and subscripts or superscripts α and β refer to the α and β relaxations, respectively. Thus N_α and N_β are the concentrations (numbers/volume) of α and β defects, μ_3 and μ_2 (for defects α and β) are the components of the dipole moments in directions z and y, respectively (see Fig. 1). Under equilibrium conditions, the quantities N_α and N_β at a given temperature are related by

$$N_\beta/N_\alpha = \exp(-\Delta g/kT), \tag{4}$$

where Δg is the difference in the binding free energy of Al–Na pair in the β and α configurations. Note, from eqn (1), that each of the four respective peak heights $\tan\delta_{max}$ is given by

$$\tan\delta_{max} = \delta\epsilon/2\epsilon_\infty, \tag{5}$$

with the respective quantities $\delta\epsilon$ coming from eqn (3). A measurable ratio that will be particularly useful later is the ratio r of the heights of the α to the β peak (both in the parallel orientation), which is equal to

$$r \equiv \frac{\delta\epsilon_{\parallel}^{\alpha}}{\delta\epsilon_{\parallel}^{\beta}} = \frac{N_\alpha}{N_\beta}\frac{T_\beta}{T_\alpha}\left(\frac{\mu_3^{\alpha}}{\mu_3^{\beta}}\right)^2, \tag{6}$$

where T_α and T_β are the two peak temperatures.

3. EXPERIMENTAL DETAILS

3.a *Crystals*

A natural crystal and various cultured crystals were used in this study. The different crystals used, with their designations and sources, are listed in Table 1. The Al content, given in the last column, was obtained

Table 1. Crystals used in this work

Designation	Source	Remarks	Al content (ppm)
GEC	General Electric (UK)	ultra pure	$\lesssim 0.1$
SQ-A	Toyo Co. (Japan)	-	13
S2	Sawyer Co. (U.S.)	-	13
NQ	Arkansas	Natural	70
HA-A	USSR	High Al	352

from the Al–Na peak heights, and the calibration which will be discussed later in this paper.

All samples obtained from cultured crystals were taken from the z-growth regions. This region is usually relatively homogeneous in its Al content. Two z-cut samples with cross section of approximately 1.5×1.5 cm^2 and thickness (parallel to the c-axis) between 1.0 and 1.8 mm were cut from each crystal. One of these samples was swept with Li^+ and the other with Na^+. (The sweeping was carried out by Dr. J. Martin at Oklahoma State University.) Unless otherwise mentioned, all samples were z-cut so that the electric field was applied parallel to the c-axis of the crystal.

3.b *Measurements*

Dielectric loss was measured using a three terminal method. The terminals were a central electrode and a concentric outer guard ring on one face of the sample, and a full electrode on the other. The diameter of the central electrode was 6.6 mm and a gap of 0.2 mm separated it from the guard ring. This configuration: guard ring width/gap width > 3, was designed to minimize fringing field effects and produce a uniform field condition [13]. Electrodes were painted on with Englehard Co. silver ink, and cured at 400°C for 15 min.

Measurements were made using a General Radio type 1620A bridge assembly. The frequency range covered extended from 20 Hz to 100 kHz.

The sample was placed inside a Janis Research Super Varitemp cryostat and connected to the bridge terminals with uninterrupted coaxial cables in order to provide continuous shielding of the leads. The shield was itself connected to the bridge ground. After cooling the sample to liquid helium temperature, measurements were made during heating at a rate ~0.01 K per 15 sec. Temperature T was monitored by reading the potential drop across a silicon diode. The uncertainty in T is ±0.05 K and the absolute error is within 0.2 K.

4. RESULTS AND DISCUSSION

4.a *Study of the Al–Na relaxations*

In several z-cut (‖ oriented) Na-swept samples, we have observed the pair of dielectric loss peaks due to Al–Na pairs. These appear at 29.8 and 75.4 K, respectively, for a frequency of 1 kHz. An example is given in Fig. 2 which compares the dielectric loss of a natural (NQ) crystal as received (unswept) with that after Li- and Na-sweeping. The two peaks are prominent in the Na-swept sample, very small in the unswept, and absent in the Li-swept sample. The locations as well as the shapes of the two peaks are precisely reproducible from sample to sample. Figure 3 illustrates this point by comparing normalized loss data for the α peak in the natural NQ and the cultured SQ crystals. It is striking that the shapes of the two peaks are so nearly identical in spite of the great difference in the origin of the crystals as well as the difference in absolute peak height, $\tan \delta_{max}$, which is six times larger for the natural crystal. A similar agreement in peak location and peak shape is found for the β peak. This kind of agreement suggests that the two peaks are unique properties of the defects involved. The respective parameters derived from the peak location, the peak width and the peak height will now be considered in turn.

Parameters of the α and β relaxations. The peak location is defined by the condition: $\omega\tau = 1$. By measuring the peak temperature at several frequencies one can, in the usual way, obtain the activation enthalpy and frequency factor of eqn (2). We have carried out such dielectric measurements in the frequency range from 1 to 10 kHz. In addition, it is well known that a corresponding pair of peaks occurs in the *acoustic* loss, usually measured at 5 MHz and appearing at 53 and 135 K, respectively [11, 12]. Although the acoustic relaxations involve different relaxational modes (the E-type) than those of the dielectric relaxation (the A_2-type), it has been shown that the τ-values of both relaxation processes are the same [9]. Accordingly, in Fig. 4 we have combined the acoustic and dielectric measurements to produce two Arrhenius plots, one for the α peak and the other for the β peak. Because of the wide range of frequencies covered when the acoustic measurements are included, it is possible to determine the quantities H and ν_0 of eqn (2) with relatively high precision. The values are given in Table 2. The lower-than-usual frequency factors ν_0 ($\sim 10^{12}$ sec^{-1}) suggest that the interstitial Na^+ moves in a shallow well in both the α and β configurations.

The width of an ideal Debye peak in reciprocal temperature units is $\delta(1/T) = 2.635k/H$ [14]. Comparing this theoretical width with the experimental one in Ta-

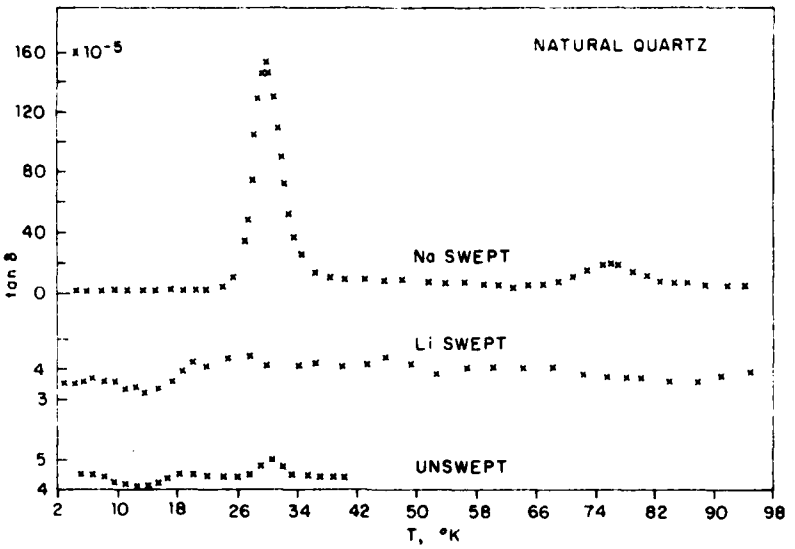

Fig. 2. Dielectric loss, tan δ, at 1 kHz of natural quartz (NQ) crystals that were unswept, Li-swept and Na-swept. Note that the scale for the two lower curves is 20× larger than that for the upper curve.

ble 2, we see that both the α and β peak widths are within 5% of the theoretical value and, as such, are among the best defined Debye-type peaks reported in the literature. The reason for the sharpness of the peaks can be related to the absence of defect interactions, probably because of the low defect concentrations and the high quality of the crystals.

As already pointed out in Section 2, eqns (3) and (5), the peak heights are related to the concentrations of defects in the two configurations, and to appropriate components of the dipole moment vector. An interesting parameter is the ratio r of the heights of the α and β peaks, given by eqn (6). Table 3 summarizes the relevant data for the various Na-swept samples studied. It is striking that the α to β ratio varies significantly among different samples, and is particularly higher for the cultured samples than for the natural (NQ) sample. It is noteworthy that the two extreme ratios, 16.8 for sample HA-A and 9.7 for NQ, were obtained after a simultaneous cooling from 100 to 4.7 K, so that the difference cannot be related to equilibration between the α and the β Al-Na defects in this low temperature range. The results of Table 3 may be compared to a ratio of 14.8 reported by Park [10] for a cultured crystal and a range of ratios from ~8 to 16 by Stevels and Volger [7].

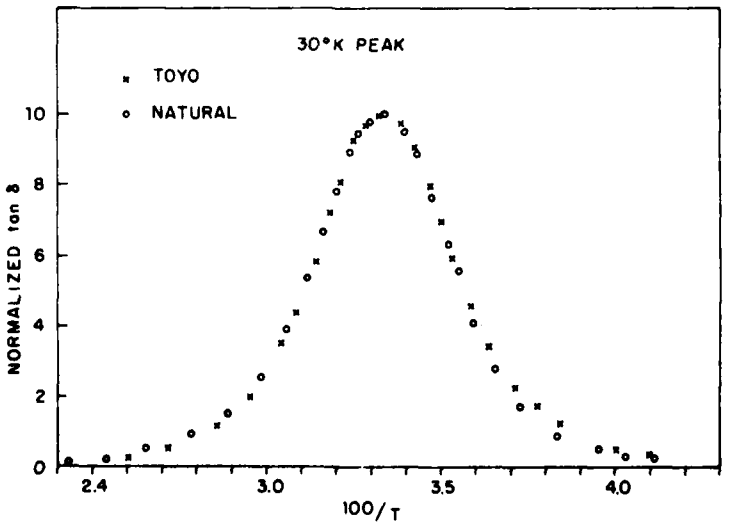

Fig. 3. Comparison of the normalized α peaks for the natural (NQ) and Toyo synthetic (SQ) Na-swept crystals. The absolute peak height is 6× higher for the NQ than for the SQ crystal. Frequency, 1 kHz.

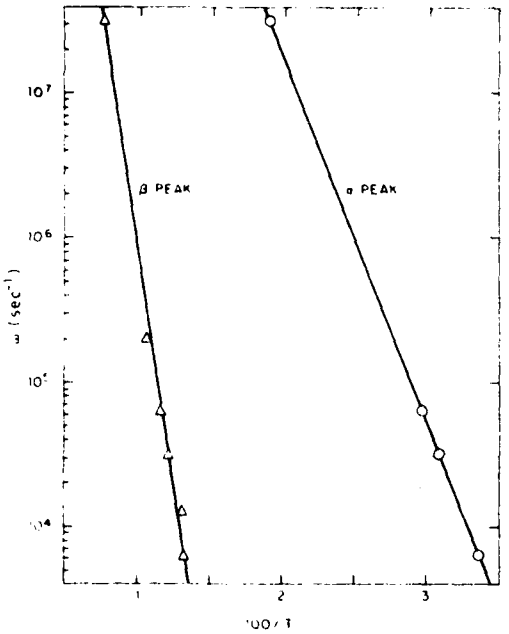

Fig. 4. Arrhenius plots (log ω vs $1/T$) for the α and β peaks, including the data from acoustic loss measurements at 5 MHz.

From the theory, it is clear that if $\alpha \leftrightarrow \beta$ equilibrium exists during the measurements, the ratio N_α/N_β should be the same for all crystals and therefore, the ratio r should be fixed. To further investigate this matter, we annealed the Na-swept samples HA-A and NQ together at 520°C for 0.5 h and then slowly cooled them to room temperture over a period of 4 h. Following this treatment, the α to β height ratio was redetermined and found to be 13.2 for HA-A and 13.7 for NQ, which may be regarded as the same within experimental error. It was also verified that the change in heights with this treatment were not compensated by any change in widths of the peaks. It is concluded, therefore, that the ratio N_α/N_β is not maintained in thermodynamic equilibrium during measurements below 100 K but is frozen in from a higher temperature (above 300 K).

We have further tested this conclusion by a careful examination of data on the β peak. If an α to β peak height ratio $\sim$ 14 corresponded to an equilibrium ratio of N_α/N_β at $\sim$75 K, then the difference in binding free energy Δg would be 0.015–0.025 eV. The estimate is readily obtained from eqn (6) and (4) allowing for reasonable values for the ratio $(\mu_3^\alpha/\mu_3^\beta)^2$. We can then use the Δg value to calculate how the height of the β peak, plotted as $T \tan \delta_{max}$, should change with temperature. In particular, for the peaks measured at 1 and 10 kHz, which appear respectively at 75.6 and 86.5 K, using even the lower estimate $\Delta g = 0.015$ eV, it is readily shown that they should differ in magnitude by more than 30%. Figure 5 shows, however, that these peak heights are the same to within experimental error ($\sim$2%), a result that is consistent with a frozen-in ratio N_α/N_β. Even more striking is the expectation that the peak must be asymmetric if N_β varies with temperature in accordance with eqn (4) as the peak is being traced out. The logarithmic plot of Fig. 5, however, shows equal slopes on both sides. In fact, if N_β were varying according to eqn (4) with $\Delta g \geq 0.015$ eV, the slope on the high temperature (low $1/T$) side of the graph would be at least 20% less steep than that on the low-temperature side, as shown by the dashed curves in the figure. The peak would then be highly asymmetrical. Figure 5 shows, however, that this is clearly not the case.

These various observations lead to the firm conclusion that the N_α/N_β ratio is frozen in from a temperature above 300 K. Let us consider the implications of this conclusion. First, it leads to an estimate of $\Delta g \geq 0.08$ eV for the difference between the α and β configurations. It also has implications for the kinetics of the various interstitial jumps. As stated earlier, the relaxation rate associated with the α peak is due to $\alpha \rightarrow \alpha$ reorientations, and is therefore controlled by the $\alpha \rightarrow \alpha$ jump. Thus the value H_α = 50 meV (see Table 2) is the activation enthalpy for this jump. The relaxation rate associated with the β peak, on the other hand, can be controlled either by direct $\beta \rightarrow \beta$ jumps or by $\alpha \leftrightarrow \beta$ jumps, whichever is more rapid [9]. If $\alpha \leftrightarrow \beta$ provided the faster jumps, however, the ratio N_α/N_β would be in thermodynamic equilibrium throughout the measurement of the β peak, in contradiction to our results. Thus, the β relaxation rate and its activation enthalpy H_β = 127 meV must be related to the $\beta \rightarrow \beta$ jump. Since the α–β equilibrium is only established at a considerably higher temperature, it must be concluded that the enthalpies for the $\alpha \rightarrow \beta$ and $\beta \rightarrow \alpha$ jumps are much larger than H_β. This conclusion can readily be understood in terms of the model of Fig. 1. Each SiO_4 tetrahedron is composed of four O^2 ions that are equivalent in pairs. Two of them form long bonds with the central Si^{4+} (or Al^{3+}) and the other two, short bonds. It is reasonable to expect that the α and β configurations involve the Na^+ ion placed on opposite

Table 2. Kinetic parameters of the α and β peaks and peak widths δ ($10^3/T$)

	H (meV)	ν_0 (sec^{-1})	$\delta(10^3/T)$ (theor.)	$\delta(10^3/T)$ (expt.)
α	50(±2)	1.1×10^{12}	4.53	4.75
β	127(±2)	1.7×10^{12}	1.78	1.80

Table 3. Peak heights of α and β peaks in various Na-swept samples (for parallel orientation)

Crystal	$\tan\delta^{\alpha}_{max}$ (10^{-5})	$r = \tan^{\alpha}_{max}/\tan^{\beta}_{max}$
HA-A	777	16.8
S 2	27.8	14.3
SQ-A	28.1	12.9
NQ	151	9.7

sides of the tetrahedron, as proposed earlier [10]. Thus, in both the $\alpha \rightarrow \alpha$ and the $\beta \rightarrow \beta$ jumps, the Na^+ moves within the relatively open c-axis channel. For the $\alpha \leftrightarrow \beta$ jumps, however, the Na^+ must cross over from one channel to the other, a much more energetic process.

These conclusions are supported by recent computer simulation calculations, which use the classical Born model with additional three-body angle-dependent terms [15]. Preliminary results show, for the Al–Na defect: (a) that there are stable α sites and β sites on opposite sides of the AlO_4 tetrahedron; (b) that α–α and β–β jumps involve low activation energies (<0.3 eV); and (c) that α–β transitions require a much higher activation energy ($\sim$1.4 eV).

Dipole moments and calibrations. In the previous discussion, we made use of the ratio r of α to β peak heights to establish the nonequilibrium status of these defects at low temperatures. Because we were able to obtain two different values of r for the same sample by different heat treatments, we are given an opportunity to estimate the quantity $\mu_3^{\alpha}/\mu_3^{\beta}$ appearing in eqn (6), and then to calibrate the Al–Na concentration in both α and β configurations.

If we denote by r and r' two values of the ratio corresponding to two different treatments of the same sample, we obtain from eqn (4):

$$r/r' = (N_{\alpha}/N'_{\alpha})(N'_{\beta}/N_{\beta}). \tag{7}$$

Further, we introduce the ratio of α peak heights for the two cases:

$$R_{\alpha} = \tan\delta^{\alpha}_{max}/\tan\delta^{\alpha'}_{max} = N_{\alpha}/N'_{\alpha} \tag{8}$$

and finally note that the total Al–Na defect concentration must be conserved at a total value N_t:

$$N_{\alpha} + N_{\beta} = N'_{\alpha} + N'_{\beta} = N_t. \tag{9}$$

Combining eqns (7)–(9) we can obtain the ratio N_{α}/N_{β}:

$$\frac{N_{\alpha}}{N_{\beta}} = \frac{(r/r')\quad R_{\alpha}}{R_{\alpha} - 1}. \tag{10}$$

The problem in utilizing eqn (10) lies in the measurement of R_{α} with sufficient precision. The best measurement that we have is for the HA–A sample, where $r = 16.8$ before heat treatment and $r' = 13.2$ afterwards. The corresponding ratio of the α peaks was $R_{\alpha} = 1.010$, the uncertainty in the quantity $R_{\alpha} - 1$ being $\sim \pm 50\%$. Inserting these values into eqn (10) gives $N_{\alpha}/N_{\beta} = 26$ and so, from eqn (6),

$$|\mu_3^{\alpha}/\mu_3^{\beta}| = 0.51\ (\pm 0.1); \tag{11}$$

i.e., the z component of the dipole moment is approximately twice as great for the β as for the α configuration. Note that, despite the very large experimental uncertainty in the quantity R_{α}, the estimated ratio $\mu_3^{\alpha}/\mu_3^{\beta}$ remains quite meaningful, due to the fact that it enters squared in eqn (6).

The result given by eqn (11) can serve as the basis for the calculation of conversion factors which allow us to obtain absolute values of N_{α} and N_{β} from the α and β peak heights. Halliburton and co-workers [16, 17] have developed a method for determining the Al content of a quartz crystal by converting it entirely into Al-hole centers through an appropriate irradiation procedure. This center has a characteristic ESR spectrum which has been calibrated. In this way, they found for an SQ–A sample, taken from the same bar as our

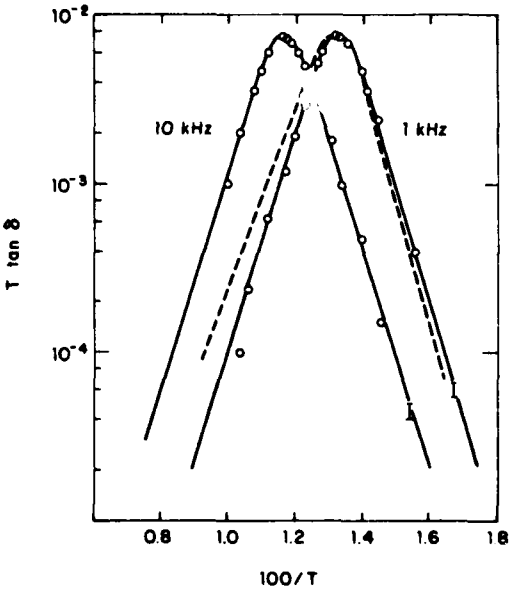

Fig. 5. Plots of $T \tan\delta$ (with background subtracted) on a logarithmic scale versus $100/T$ for the β peak in a Na-swept crystal at 1 and 10 kHz. The dashed curve for the 1 kHz case is calculated under the assumption that the enthalpy difference between the α and β states is 0.015 eV and that α–β equilibrium is always maintained. Under this same assumption the 10 kHz peak should be at least $\sim$30% higher than the 1 kHz peak.

sample, a value of 12.8 ± 0.6 ppm Al. Because of the homogeneity of the z-growth region from which these samples were taken, and because of the proven effectiveness of the sweeping procedure, we can assume that our Na-swept SQ–A sample possessed the same Al content, entirely in the form of Al–Na pairs. In this case we have

$$C_\alpha + C_\beta = C_t = 12.8 \text{ ppm},$$

where the symbol C refers to concentration expressed as a mole fraction (i.e. relative to the total Si concentration). Using the ratio of dipole moments given by eqn (11) and the ratio of peak heights $r = 12.9$ (see Table 3), we obtain $C_\alpha/C_\beta = 19.8$. From the sum and the ratio of C_α and C_β, we obtain $C_\alpha = 12.2$ ppm and $C_\beta = 0.62$ ppm. Knowing the heights of the two dielectric loss peaks for the Na-swept SQ–A sample, we derive finally at the following calibrations:

$$\left.\begin{aligned} C_\alpha \text{ (ppm)} &= (0.43 \pm 0.02) \times 10^5 \tan \delta^\alpha_{\max}, \\ C_\beta \text{ (ppm)} &= (0.29 \pm 0.10) \times 10^5 \tan \delta^\beta_{\max}. \end{aligned}\right\} \quad (12)$$

Note that the uncertainty in the calibration of the β peak is large due to the large uncertainty in $(\mu_3^\alpha/\mu_3^\beta)^2$.

A more practical calibration is to relate just the α peak height to the *total* Al–Na concentration, since the α peak is the much larger one and it is more easily used to monitor the Al–Na content. Strictly, the result depends on the α/β ratio r, but variations in r produce only small changes in that calibration. Thus, taking $r = 13$ as an average value, we obtain

$$C_t \text{ (ppm)} = (0.45_5 \pm 0.03) \times 10^5 \tan \delta^\alpha_{\max}, \quad (13)$$

which is not very different from the result for C_α in eqn (12), since $C_\beta \ll C_\alpha$. Since an α peak height of 1×10^{-5} is observable (see, e.g., the data for the unswept sample in Fig. 2), one concludes that as few as 0.5 ppm of Al–Na centers may be detected by this method.

Using the calibration constants of eqn (12) together with eqns (1) and (3) and the requirement that $\omega\tau = 1$ at the peak, enables us to obtain the dipole moment as components μ_3^α and μ_3^β, as follows:

$$\left.\begin{aligned} \mu_3^\alpha &= 5.4 \times 10^{-30} \text{ C–m}, \\ \mu_3^\beta &= 10.5 \times 10^{-30} \text{ C–m}. \end{aligned}\right\} \quad (14)$$

If we then simply set $\mu_3 = ez$, where e is the electronic charge and z the separation of charge in the z direction, we obtain: $z^\alpha = 0.34$ A and $z^\beta = 0.66$ A.

Equation (3) shows that the components μ_2^α and μ_2^β can be similarly obtained from measurements on samples oriented perpendicularly to the c-axis. Such measurements were made by Park [10] who showed that the anisotropy ratio $(\delta\epsilon_\parallel/\delta\epsilon_\perp)$ for both the α and β peaks is ~30. Accordingly, from eqn (3) we may obtain the y components of the defect dipole moment, giving $y^\alpha = 0.10$ A, $y^\beta = 0.18$ A. The dipole components μ_1 are not obtainable from dielectric relaxation measurements, since this is the component along the symmetry (C_2) axis (see Fig. 1) which is unchanged during any α–α or β–β jump of the Na^+ ion. Nevertheless, considering that the ionic radii of Al^{3+} and Na^+ are 0.51 and 0.97 A, respectively, the numbers obtained for y and z components are clearly too small.

The result that, if the dipole moment μ is interpreted as electronic charge multiplied by distance $\mathbf{r}$, the magnitude of that distance comes out too small, is actually a common problem in dielectric relaxation. Attempts to deal with it by introducing an internal field correction [7] have not been particularly successful. The reason for these problems is that the proper definition of μ is given in macroscopic rather than atomistic terms. Specifically, the components of μ are properly defined in terms of an extra electric polarization per unit excess concentration of defects in a given orientation [8]. It therefore does not follow that the μ values so obtained will come out to be simply the bare dipole moment, i.e. e times the actual defect dimensions, except in order of magnitude. (Also see [18].) The relative values of these components, however, may be regarded as providing meaningful information on the coordinates of the Na^+ ion about the AlO_4 tetrahedron.

4.b *Search for Al–Li relaxations*

In view of the usefulness of the Al–Na loss peaks to characterize the Al–Na defect pair and to monitor the Na content, we have attempted to find similar peaks due to Al–Li pairs. We have accordingly examined a variety of unswept and Li-swept samples, both z-cut and x-cut, over the entire range from 2.9 to 290 K.

In all of these experiments, no identifiable peak was found, in contrast to Stevels and Volger's claim [7] of a Li peak at 60 K for a frequency of 32 kHz. The middle curve of Fig. 2 shows one of the better examples of this search. For this Li-swept natural crystal with an Al content as high as 70 ppm, there is no sign of any peak greater than 0.5×10^{-5}. Even the small fluctuations that appear in Fig. 2 were shown by repeated experiments to be random and strictly part of the background losses. It is noteworthy that a recent study of anelastic loss at 5 MHz also finds no peaks for Li-swept crystals over a similar temperature range [12].

There is little doubt that Al–Li pairs are present, i.e. that the sweeping was successful, since there are no traces of Al–Na relaxations or of Al–OH infrared absorptions in such Li-swept samples. In view of the high Al content of the samples studied, it follows that the values of μ_2 and μ_3 that must be assigned to the Al–Li defect are at least one order of magnitude smaller than the values for the Al–Na pair. The most reasonable conclusion is that these components are precisely zero, i.e. that the Li^+ ion resides on the C_2 axis of the distorted SiO_4 tetrahedron. The absence of relaxation is then due to the fact that there is no possibility for reorientation under an applied electric field. It is probably because of the small size of the Li^+ ion (radius 0.68 Å) that it can reside on the C_2 axis between two oxygen ions and closer to the Al^{3+} than the Na^+ ion. Conse-

quently, we may expect that the binding energy of the Al–Li pair should be higher than that of the Al–Na pair.

Interestingly enough, a recent computer simulation study [15], already mentioned earlier, has shown that, whereas the Na^+ sits off of the C_2 axis of the AlO_4 tetrahedron, the Li^+ resides on this axis. Furthermore, the binding energy of the Al–Li pair is about 0.45 eV higher than that of the Al–Na pair.

It is satisfying that, in this case, a negative experimental result has led to definite information about the structure of the Al–Li defect. However, the absence of a characteristic peak is disappointing, since it leaves us without a means for directly monitoring the Al–Li content of crystals. Such a monitor would be most valuable in view of the fact that today's higher quality cultured quartz crystals are grown with Li^+ in the mineralizer, and consequently with Al^{3+} associated predominantly with Li^+ in the crystal.

5. CONCLUSIONS

In this section, we summarize what has been learned in this work concerning both the Al–Na and Al–Li defects.

Al–Na defect

The appearance of α and β peaks are a result of the existence of distinct α and β configurations for this defect. The α relaxation is controlled by $\alpha \rightarrow \alpha$ jumps with $H \simeq 50$ meV and the β relaxation by $\beta \rightarrow \beta$ jumps with $H \simeq 127$ meV. The frequency factors in both cases are close to 10^{12} sec^{-1}. Both peaks are very nearly single Debye relaxations.

The β/α ratio is frozen in the vicinity of the β peak (near 100 K), showing that the $\alpha \rightarrow \beta$ jump requires a high activation enthalpy, probably >1 eV. This suggests that the α and β configurations involve the Na^+ ion located on opposite sides of the AlO_4 tetrahedron.

The ratio of z-components of the dipole moments is $|\mu_3^{\alpha}/\mu_3^{\beta}| \cong 0.5$. On this basis, and with the aid of information from EPR measurements following irradiation, it has been possible to calibrate the heights of the α and β peaks, as given by eqn (12).

Al–Li defect

The absence of relaxations (both dielectric and anelastic) in Li-swept crystals leads to the conclusion that, in contrast to the case of Na^+, Li^+ sits on the C_2 axis of the AlO_4 tetrahedron.

Acknowledgements—The authors are grateful to Professor Joel Martin for carrying out the electrodiffusion on the various samples studied herein. This work was supported by the U.S. Air Force under contract F 19628-82-K-0013 and monitored by H. G. Lipson, RADC Hanscom AFB.

REFERENCES

1. Kats A., *Philips Res. Rep.* **17**, 133 (1962).
2. Brown R. N. and Kahan A., *J. Phys. Chem. Solids* **36**, 467 (1975).
3. Lipson H. G., Euler F. and Armington A. F., *Proc. 32nd Ann. Frequency Control Symp.*, p. 11. USAERADCOM (1978).
4. King J. C., *Bell Syst. Tech. J.* **38**, 573 (1959).
5. King J. C. and Sander H. H., *Rad. Effects* **26**, 203 (1975).
6. Capone B. R., Kahan A., Brown R. N., and Buckmelter J. R., *IEEE Trans. Nucl. Sci.* **NS-13**, 130 (1966).
7. Stevels J. M. and Volger J., *Philips Res. Rep.* **17**, 283 (1962).
8. Nowick A. S. and Heller W. R., *Adv. Phys.* **14**, 101 (1965); **16**, 1 (1967).
9. Nowick A. S. and Stanley M. W., in *Physics of the Solid State* (Edited by S. Balakrishna), p. 183. Academic, New York (1969).
10. Park D. S. and Nowick A. S., *Phys. Status Solidi* (a) **26**, 617 (1974).
11. Fraser D. B., in *Physical Acoustic* (Edited by W. P. Mason), *Vol. 5, Chap. 2.* Academic, New York (1968).
12. Martin J. J., *J. Appl. Phys.* **56**, 2536 (1984).
13. Andeen C., Fontanella J. and Schuele D., *Rev. Sci. Instrum.* **41**, 1573 (1970).
14. Nowick A. S. and Berry B. S., *Anelastic Relaxation in Crystalline Solids*, Chap. 3. Academic, New York (1972).
15. Leslie M. and Catlow C. R. A., private communication.
16. Markes M. E. and Halliburton L. E., *J. Appl. Phys.* **50**, 8172 (1979).
17. Halliburton L. E., Koumvakalis N., Markes M. E. and Martin J. J., *J. Appl. Phys.* **52**, 3565 (1981).
18. Franklin A. D. and Lidiard A. B., *Proc. R. Soc. London Ser A* **392**, 457 (1984).

EFFECT OF ALKALI IONS ON ELECTRICAL CONDUCTIVITY AND DIELECTRIC LOSS OF QUARTZ CRYSTALS*

J. Toulouse, E.R. Green and A.S. Nowick
Henry Krumb School of Mines
Columbia University, New York 10027

Summary

Because of the importance of alkali ions in relation to frequency stability of quartz resonators, we have investigated the electrical properties of various Li-swept and Na-swept quartz crystals (both natural and synthetic). These properties are of two types: dielectric loss measurements, particularly at cryogenic temperatures, and electrical conductivity measured between 100° and 400°C. In the case of the dielectric measurements, we studied the two well known loss peaks due to Al-Na pairs and established a calibration for the lower temperature peak (tan δ_{max} of 1.5×10^{-5} corresponding to 1 ppm of Al-Na pairs). High quality synthetic crystals and a natural crystal were found to have primarily Li as compensation for Al in the as-grown condition. The absence of an analogous Al-Li peak leads to the conclusion that Li resides on the 3-fold symmetry axis of the AlO_4 tetrahedron to which it is bound. Following irradiation, large loss peaks were found, at 8.4 K for Na-swept and at 6.85 K for Li swept crystals. These peaks may be useful to characterize quartz crystals.

The ionic conductivity is different for Na and Li in the same crystal, and also for synthetic and natural crystals. Conductivity is controlled by a combination of the energy of migration of free M^+ and of association of the Al-M pair.

Introduction

It is well established that frequency instabilities in quartz resonators, especially after irradiation, are related to impurities in the crystals.[1-4] Probably the most important impurity is Al^{3+} substituting for Si^{4+}, which (due to its lower valence) requires an additional defect for charge compensation. The latter is most commonly an interstitial monovalent ion, M^+, notably the alkalis, Li^+ and Na^+, or hydrogen. Because of the Coulombic attraction between the M^+ and the Al^{3+} (which carries an effective charge of -1), the M^+ interstitial is usually located adjacent to the Al^{3+} ion at low to moderate temperatures.

Two types of electrical properties provide useful ways to observe the effects of alkali ions; these are dielectric loss, and conductivity. The pioneering work of Stevels and Volger[5] showed that dielectric loss (or "dielectric relaxation") observed at cryogenic temperatures showed a number of peaks, two of which could be attributed to Al-Na pairs. Subsequent work in this laboratory[6,7] showed that a Na^+ ion can occupy two pairs of equivalent sites (a total of 4 sites), which may be considered nn and nnn positions, about a given AlO_4 tetrahedron. An electric field gives rise to dielectric loss by producing preferential reorientation between an equivalent pair of sites, the lower temperature loss peak being due to nn reorientation and the higher temperature one to nnn reorientation. Analogous acoustic loss (or "anelastic relaxation") peaks are also known.[8]

An important question is whether there are similar loss peaks due to Al-Li pairs. Such a peak was claimed by Stevels and Volger[5] to be present at 60 K (for a frequency of 32 kHz). There is a need to confirm this claim, since such a peak would provide a valuable method for characterizing the Li^+ content of quartz crystals.

The second property of interest is electrical conductivity. Because of the large band gap of crystalline quartz (~ 8 eV) such conductivity is entirely ionic, and is due to alkali ions that have broken away from Al-M pairs as a consequence of the dissociation equilibrium. A detailed study by Jain and Nowick[9] has shown some interesting differences between natural and synthetic crystals, in particular, a lower activation energy for natural crystals.

Both electrical properties are strongly dependent upon the morphology of the alkali defect, which can be modified by irradiation.[10] Therefore we have also begun to investigate the effects of X-irradiation upon dielectric loss and conductivity.

In order best to study these electrical properties related to alkalis, it is desirable to obtain crystals that have Al compensated by just one alkali at a time. This objective can be met by the process of electrodiffusion (or "sweeping"), i.e. application of an electric field parallel to the z-axis to introduce the desired interstitial ion into the lattice replacing those that were grown in. This method was previously developed by Kats[11] and by King[1] and is now a relatively standard technique. In addition to alkalis, H^+ can also be swept into the crystal. By studying the electrical properties of Li-, Na- and H-swept crystals we hope to achieve a better understanding of these properties than had been achieved in the past with measurements on various as-grown crystals.

Experimental

The principal synthetic crystals studied were high quality crystals taken from the Z-growth region: Toyo Supreme Q (bar SQ-A) and Sawyer Premium Q (bar PQ-E). The natural crystal was a clear crystal from Arkansas.

Electrodiffusion experiments were carried out at Oklahoma State University by Dr. J. Martin. (Method described in ref. 12). Dielectric loss (tan δ) and ionic conductivity were both measured with a General Radio type 1620A Capacitance Bridge assembly over the frequency range 20 Hz-100 kHz. Complex impedance analysis was used to obtain the bulk conduction.[9] The samples used were plates of surface area 1 cm^2 and thickness 1.0-1.5 mm coated with sputtered silver electrodes. Most samples were cut so that the electric field is applied parallel to the z-axis, but some were

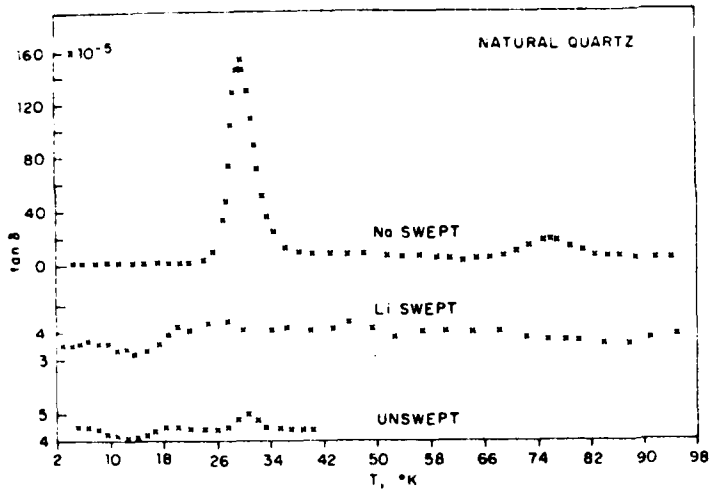

Fig. 1. Dielectric loss of natural quartz crystals that were unswept, Li-swept and Na-swept. Note that the scale for the two lower curves is 20 x larger than that for the upper curve.

cut in a perpendicular orientation. The sample chamber for the conductivity measurements was described previously.[9] For dielectric loss, the sample was inserted into a Janis Supervaritemp cryostat, and measurements were taken between 2.9 and 300 K. The leads from the bridge to the sample electrodes were shielded by a continuous coaxial shield connected to the bridge ground.

X-irradiation was carried out for 4 hours at room temperature using a conventional tungsten-filament tube at 40 kV and 20 mA. The very soft X-rays were filtered out by the layer of sputtered silver used as electrodes.

Dielectric Relaxation Studies

The Al-Na Peaks

In several samples containing Na, we have observed the pair of peaks previously reported by Stevels and Volger[5] and by Park[7] as due to Al-Na pairs. At a frequency of 1 kHz these peaks appeared at 30 K and 75 K. An example is given in Fig. 1 which compares dielectric loss (tan δ) for the natural crystal as received (unswept) and after Li-and Na-sweeping. The two peaks are prominent in the Na-swept sample, very small in the unswept and absent in the Li-swept sample. The 30 K peak is especially interesting as a very sensitive measure of the Al-Na content just as is the 50 K anelastic peak (at 5 MKz).[8,13] In fact, by comparing the temperature location of the dielectric peak at 1 kHz with that of the anelastic peak at 5 MHz, one obtains H = 0.052 eV as the activation enthalpy of the peak. Figure 2 shows a more detailed examination of the peak shape, comparing normalized data for the natural and the Toyo synthetic crystal. It is striking that the shapes are so nearly identical (except for a possible small tail on the high 1/T side for the synthetic crystal) in spite of the great difference in origins of these two crystals and a peak height that is 7x larger for the natural crystal. From the peak width of Fig. 2 an apparent activation energy of 0.050 eV is obtained, showing that the peak is only 4% wider than a perfect Debye peak.[14] This relaxation peak is attributed[6,7] to reorientation between the two equivalent nn configurations of the Al-Na pair. A similar agreement in peak shapes between natural and synthetic is found for the 75 K peak, which is attributed to nnn Al-Na pairs.

The study of the Toyo Supreme SQ-A sample allows a calibration of the 30 K peak. Halliburton et al.[15,10] developed a method for determining the Al content of a quartz crystal by converting all of it to Al-hole ($Al\text{-}h^+$) centers through an appropriate irradiation procedure; these centers could then be detected and their concentration determined through ESR measurements. In this way, they found, for an SQ-A specimen from the same bar as our sample, a value of 14.4 ppma of Al. If we assume that our Na-swept SQ-A sample contained the same Al content and that the Na sweeping converted all Al to Al-Na defects, then our peak height tan δ_{max} of 22.1×10^{-5} must correspond to 14.4 ppm of Al-Na defects. This result then gives a calibration constant of 1.5×10^{-5}/ppm.

The earlier theoretical treatment[6] permits us to interpret this calibration constant. It was shown that the relaxation strength $\delta\epsilon_{//}/\epsilon_{//}$ of the dielectric constant $\epsilon_{//}$ parallel to the z-axis is given by

$$\frac{\delta\epsilon_{//}}{\epsilon_{//}} = 2 \tan \delta_{max} = \frac{n_d \mu_3^2}{kT} \qquad (1)$$

where tan δ_{max} is the measured peak height, n_d the number of dipoles (Al-Na pairs) per unit volume, μ_3 the component of the dipole moment parallel to the z-axis and kT has its usual meaning. The above calibration constant then gives a value of $\mu_3 \sim 5 \times 10^{-30}$ C-m, or a charge separation $r_3 \sim 0.3$ A, which is reasonable.

Table 1 presents a summary of the results for the 30 K peak for a variety of samples that we have studied (all measured parallel to the z-axis). In the final column this calibration constant is used to convert peak heights into concentration of Al-Na pairs. It is interesting that these high quality synthetic crystals (SQ-A and PQ-E), grown with Li^+ in the mineralizer, show only a very small amount of Na in the as-grown condition. The total Al content of the PQ-E crystal, for example was ~ 18 ppm;[10] therefore, only 4% of the Al^{3+} is associated with Na in the as grown condition. Similarly there is only 15% Al-Na in the Toyo SQ-A crystal. The remainder is almost certainly Al-Li, since there is no evidence in these crystals for infrared absorption due to Al-OH centers.[16]

Table 1. Results for the 30 K peak for various samples

Sample	Peak height $\tan \delta_{max} \times 10^5$	ppma Na
SQ-A unswept	3.2	2.1
SQ-A Na-swept	22.1	14.4
PQ-E unswept	1	0.7
NQ unswept	1	0.7
NQ Na-swept	151	100

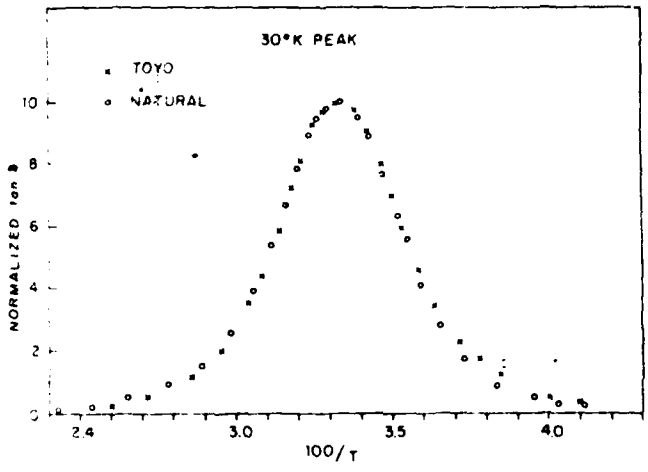

Fig. 2. The 30 K dielectric loss peak on a normalized plot for: ○ the natural crystal, × the Toyo SQ-A crystal. (The absolute peak height of the natural is 7 x higher that that of the Toyo crystal.)

Search for Al-Li Peaks

In attempting to find one or more dielectric loss peaks due to Al-Li pairs, we have examined several unswept and Li-swept samples both parallel and perpendicular to the z-axis and over the temperature range 2.9 - 290 K. In all of these experiments no identifiable peak was found, in contrast to Stevels and Volger's claim of a peak at 60 K (for 32 kHz). The middle curve of Fig. 1 shows one of the best examples, that of a Li-swept natural crystal. In this case, for which the Al content is 100 ppm (see Table 1) there is no evidence for a peak as large as $\tan \delta_{max} = 1 \times 10^{-5}$. (Even small fluctuations which might hide very small peaks in Fig. 1 were later shown, by remeasurement, not to be peaks.) Thus, using Eq. (1), if a Al-Li peak exists for measurements parallel to the z-axis, it must correspond to a value of μ_3 at least an order of magnitude smaller than that for Al-Na. Similarly, measurements with electric field in the basal plane, for which the corresponding relaxation-strength equation is[6]

$$\delta\varepsilon_1/\varepsilon_1 = 2 \tan \delta_{max} = n_d \mu_2^2/2kT \qquad (2)$$

where μ_2 is the component of dipole moment in the y-direction of the crystal, again gave negative results, suggesting that μ_2 is also exceedingly small. It is noteworthy that anelastic relaxation, which involves the same relaxational mode[6] as ε_1, is also absent for Li-swept crystals over a similar temperature range.[13]

It is therefore concluded that the Al-Li pair is most likely oriented along the x-axis, i.e. the direction of the 2-fold (C_2) symmetry axis of the crystal, as shown in Fig. 3. Because Li^+ locates itself on this axis, the two equivalent sites between which reorientation occurs in the case of Na^+, have now collapsed into a single site; thus, the possibility for reorientation, i.e. for dielectric relaxation, no longer exists. [This last remark is just a restatement, in physical terms, of what is contained mathematically in Eqs. (1) and (2).] A possible explanation for the orientation of the Al-Li pair along the C_2 axis may be related to the small size of the Li^+ ion which may permit it to sit between two oxygen ions of the AlO_4 tetrahedron. On the other hand, the Na^+ ion is believed to prefer to form an O-Na type of bond with one of the four oxygen ions of the tetrahedron.[7] One way to explore the defect configurations further is by computer simulations using the HADES II type program.[17] Such methods have given insight into the minimum-energy configurations of different defect clusters in a variety of ionic crystals and may also be useful in the present case.

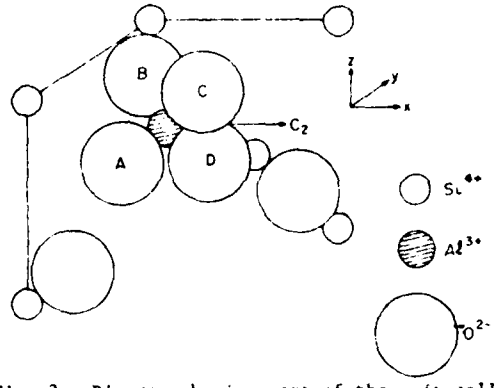

Fig. 3. Diagram showing part of the unit cell of α-quartz containing a substitutional Al^{3+} that forms an AlO_4 distorted tetrahedron. The two-fold symmetry axis, C_2, which lies parallel to the x-axis, is also shown.

Irradiation Peaks

X-irradiation produces a large peak at very low temperatures, with a high rising background below the peak. Figure 4 shows the results for Toyo Supreme SQ-A samples that had been Li-, Na- and H-swept. In the Na-swept case, the 30 K (100/T = 3.3) Al-Na peak is considerably reduced and replaced by a huge peak at 8.4 K with a rising background at still lower temperatures. A similar peak is present for the Li-swept case, but it is located at a lower temperature, 6.85 K. The H-swept sample, on the other hand, shows a smaller less well-defined peak after irradiation, which might be interpreted as a composite of the residue of the peaks for the Li-and Na-swept samples.

It is reasonable to ascribe these radiation induced peaks either to the Al-h^+ center or to a center that involves the alkali. The fact that the peaks for the different alkalis have different temperatures and that the H-swept sample shows a lower and less well defined peak suggests the possibility of an alkali center. A simple M-$\bar{e}$ center is not very likely, since such a center with a single electron would have a strong ESR spectrum, yet has not been detected in irradiated samples.[18] A more complex alkali center may be involved; for example, it may contain two electrons and possibly an oxygen-ion vacancy. More work is clearly needed to further explore these interesting irradiation induced peaks as well as the very low-temperature background effect which accompanies them.

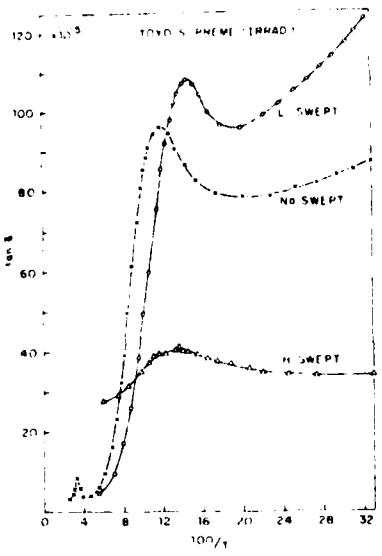

Fig. 4. Dielectric loss of three differently swept Toyo SQ-A samples following X-irradiation.

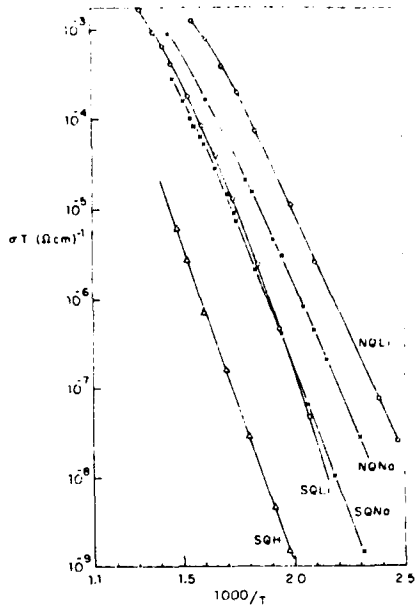

Fig. 5. Conductivity plots (log σT versus 1/T, where σ is the conductivity) for Li- and Na-swept natural quartz samples (NQ), and for three differently swept synthetic samples (Toyo SQ-A). The corresponding activation energies are given in Table 2.

Conductivity Studies

Conductivity measurements were carried out on unswept and swept Toyo SQ-A and natural crystals. All measurements were made with electric field parallel to z-axis. The results, shown in Fig. 5, are somewhat different for the two types of quartz. For the natural crystal, the Li-swept shows a substantially higher conductivity and a slightly lower activation energy (see Table 2). On the other hand, for the Toyo synthetic crystal, the conductivities are quite close and the Li-swept has the higher activation energy. Also included in Fig. 5 are results for the H-swept Toyo crystal. Here the conductivity has dropped by more than two orders of magnitude, yet the activation energy is comparable to that of the alkali swept crystals. It is therefore reasonable to regard that the conductivity of H-swept sample is not due to H^+ migration, but to the small amount of residual alkali which remains after sweeping.

Table 2. Activation Energies from Conductivity Measurements.

Crystal	Sweeping	E(eV)
Natural NQ	Li	1.09
Natural NQ	Na	1.11
Toyo SQA	Li	1.44
Toyo SQA	Na	1.31
Toyo SQA	H	1.43

Table 2 also shows that the activation energies for both natural crystals fall well below those for the synthetics, as Jain had already observed.[9] These differences were interpreted in terms of the relation.

$$E = E_m + \beta E_A \qquad (3)$$

where E_m is the activation energy for migration of a free alkali ion, E_A is the Al-M association energy, and β can vary between $\frac{1}{2}$ and 1 with the value of unity for synthetic crystals, in which the defect concentrations are so small that additional unassociated Al may be present. In any case, the term E_A dominates the expression for E, so that a higher value for Li^+ than for Na^+ does not mean that the larger (Na^+) ion migrates down the open channels of the crystal more rapidly than the small Li^+ ion. Rather, because of the small size of Li^+, it is possible that E_A for Al-Li is higher than that for Al-Na.

Conclusions

Li^+ and Na^+ behave quite differently in their effects on (*i*) dielectric loss, (*ii*) dielectric loss after irradiation and (*iii*) electrical conductivity. The first of these properties involves the bound Al-M pair; this study has shown that the two alkalis sit on very different sites. The second property may tell us what becomes of the alkali ion during irradiation, information which has thus far not been revealed by other methods. The third property is controlled by free M^+ ions produced by the dissociation of pairs; it involves both the energy of migration and of association. In each category, understanding the difference between Li^+ and Na^+ can help us better to characterize quartz crystals and to understand the origin of frequency instabilities.

Acknowledgements

The authors are grateful to Prof. Joel Martin for carrying out electrodiffusion on the samples studied here, and to Prof. L. Halliburton for helpful suggestions. This work was supported by the U.S. Air Force under contract F 19628-82-K-0013.

References

1. J.C. King, Bell Syst. Tech. J. 38, 573 (1959).
2. B.R. Capone, A. Kahan, R.N. Brown and J.R. Buckmelter, IEEE Trans. on Nucl. Sci. NS-17, 217 (1970).
3. J.C. King and H.H. Sander, Radiation Effects 26, 203 (1975).
4. R. Euler, H.G. Lipson and P.A. Ligor, Proc. 34th Annual Symp. on Freq. Control (ASFC), 72 (1980).
5. J.M. Stevels and J. Volger, Philips Res. Rep. 17, 283 (1962).
6. A.S. Nowick and M.W. Stanley, in Physics of the Solid State, S. Balakrishna, editor, Academic Press, N.Y., 1969, p. 183.
7. D.S. Park and A.S. Nowick, Phys. Stat. Sol. (a) 26, 617 (1974).
8. D.B. Fraser, in Physical Acoustics, Vol. V, W.P. Mason, editor, Academic Press, N.Y., 1968, Chapter 2.
9. H. Jain and A.S. Nowick, J. Appl. Phys. 53, 477 (1982).
10. L.E. Halliburton, N. Koumvakalis, M.E. Markes and J.J. Martin, J. Appl. Phys. 52, 3565 (1981).
11. A. Kats, Philips Res. Repts. 17, 133 (1962).
12. J.J. Martin, L.E. Halliburton, R.B. Bossoli and A.F. Armington, Proc. 36th ASFC, 77 (1982).
13. J.J. Martin, L.E. Halliburton and R.B. Bossoli, Proc. 35th ASFC, 317 (1981).
14. A.S. Nowick and B.S. Berry, Anelastic Relaxation in Crystalline Solids, Academic Press, N.Y., 1972, Chapter 3.
15. M.E. Markes and L.E. Halliburton, J. Appl. Phys. 50, 8172 (1979).
16. J.J. Martin, private communication.
17. W.C. Mackrodt, in Computer Simulation of Solids, C.R.A. Catlow and W.C. Mackrodt, editors, Springer-Verlag, Berlin, 1982, Chapter 12.
18. L.E. Halliburton, private communication.

DIELECTRIC LOSS IN Li- AND Na-SWEPT α-QUARTZ AND THE EFFECT OF IRRADIATION

J. TOULOUSE AND A.S. NOWICK
Henry Krumb School of Mines, Columbia University,
New York, New York 10027.

ABSTRACT

Alkali ions, which compensate for substitional Al^{3+}, play an important role in the frequency stability of α-quartz crystals. In this work, low temperature dielectric-loss measurements (between 2.9 and 300 K) are carried out on crystals that have been "swept" so as to introduce either Li^+ or Na^+. High quality synthetic crystals as well as natural crystals are employed. The well known loss peaks due to Al-Na pairs are further explored and similar peaks due to Al-Li are sought after but not found. It is concluded that the Al-Li pair is oriented along the C_2-axis of the AlO_4 distorted tetrahedron. After irradiation, large peaks are observed at very low temperatures both in Li^+- and Na^+-containing crystals. These peaks, which are distorted below ~6 K due to the onset of quantum effects, may originate in alkali centers produced when alkali ions are liberated by the irradiation.

INTRODUCTION

Quartz-crystal controlled resonators are widely used where there are severe requirements of frequency stability, e.g. in communications and guidance systems. [1] For such applications there is great interest in the origins of frequency instability, both in the presence and absence of radiation environments. Such frequency instabilities are usually traced to the presence of point defects in the crystals and to changes in the configurations of such defects. [2,3]

An important defect in α-quartz crystals is Al^{3+} substituting for Si^{4+} and electrically compensated by an alkali, M^+, or hydrogen, H^+, in a nearby interstitial site. Information about these defects has been obtained from a variety of physical techniques. Thus, infrared absorption measurements reveal the presence of OH^- stretching vibrational modes, with different peak locations for different environments of the OH^- bond [4,5] In particular, there are two IR bands (at 3306 and 3367 cm^{-1}) known to be related to an OH^- adjacent to a substitutional Al^{3+}. [5,6] The presence of associated Al-Na pairs has been shown to give rise to low-temperature dielectric loss peaks [7,8] as well as to anelastic loss (internal friction) peaks. [9] Electrical conductivity measurements have been used to study alkalis liberated thermally from Al-M pairs at elevated temperatures. [10] Finally, electron spin resonance (ESR), which only detects defects possessing unpaired electrons, has been most useful after irradiation. [11] It has most prominently focused on the aluminum-hole (Al-h^+) center and demonstrated that irradiation above ~250 K results in the liberation of alkali ions from the Al-M pair. [12]

An important advance has been the ability to replace one M^+ ion by another through electrodiffusion or "sweeping". [13,9] This technique consists in applying an electric field parallel to the c-axis of the crystal in the temperature range of 400-550°C. If a Li^+ or Na^+ salt is present at the anode, that ion will be swept into the crystal and replace existing M^+ ions. On the other hand, sweeping carried out either in air or in hydrogen replaces alkalis by H^+ ions.

Mat. Res. Soc. Symp. Proc. Vol. 24 (1984)

The present paper attempts to extend further the use of low-temperature dielectric loss measurements, especially with swept samples containing one of the alkali species (either Li^+ or Na^+) at a time. Both unirradiated and X-irradiated crystals are investigated.

EXPERIMENTAL METHODS

Dielectric loss measurements were performed primarily on clear natural quartz from Arkansas and high quality synthetic quartz from the Toyo company. Samples from these two sources were electrodiffused (swept) with lithium, sodium and hydrogen separately, by Dr. J. Martin at Oklahoma State University. In the case of the alkalis, chloride salts are applied on the surfaces of the samples which are then placed in an electric field of several V/cm. Hydrogen sweeping is carried out in a hydrogen atmosphere under much larger electric fields. For irradiation, samples were exposed to X-rays from a tungsten target source. The X-ray tube was operated at 20 mA and 40 kV and the irradiations lasted four hours (a dose $\sim 10^6$–10^7 rads).

After preparation, the samples were placed inside a Super Varitemp (Janis Corp.) cryostat and cooled down to liquid helium temperature. Measurements were then taken upon heating at a rate of approximately 1/100 K per 15 sec. Temperatures were monitored through the voltage drop appearing across a silicon diode. The uncertainty in temperature is ±0.05 K, while the absolute error is within 0.2 K.

The dielectric loss measurements were made using a General Radio 1615 A bridge assembly. The sample was part of an electrical circuit with a continuous shield connected to the bridge ground.

All crystals were cut and measured parallel to the c-axis except where otherwise mentioned.

RESULTS AND DISCUSSION

Unirradiated Crystals

The Na-swept crystals presently studied show the pair of low-temperature dielectric loss peaks, previously reported by Stevels and Volger [7] and by Park [8], which are attributed to Al-Na pairs. At a frequency of 1 kHz these peaks appear at 30 K and 75 K. An example is given in Fig. 1 which compares dielectric loss ($\tan\delta$) for the natural (NQ) crystal as received (unswept) and after Li- and Na-sweeping. The two peaks are prominent in the Na-swept samples, very small in the unswept and absent in the Li-swept sample. The 30 K peak is especially interesting as a very sensitive measure of the Al-Na content. Figure 2 shows a detailed examination of the peak shape of the 30 K peak, comparing normalized data for the Na-swept synthetic (SQ-A) and natural (NQ) crystals. It is striking that the shapes are nearly identical (except for a possible small tail on the high 1/T side for the synthetic crystal) in spite of the great difference in origin of these two crystals and a peak height that is 7 times larger for the natural crystal.

To the 30 K peak observed by dielectric loss measurements there corresponds a 53 K anelastic peak at 5 MHz. [9,14] By comparing the temperature location of the dielectric peak at 1 kHz with that of the anelastic peak at 5 MHz, one obtains the value $H_r = 0.051$ eV for the activation enthalpy, and $\nu_0' = 2 \times 10^{12}$ sec^{-1} for the pre-exponential in the Arrhenius expression,

$$\tau^{-1} = \nu_0' \exp(-H/kT) \qquad (1)$$

for the relaxation time τ. From the peak width of Fig. 2, an apparent

activation enthalpy of 0.049 eV is obtained, showing that the peak is only 4% wider than a perfect Debye peak. [15] A similar agreement in peak shapes between the natural and synthetic crystal is found for the 75 K peak.

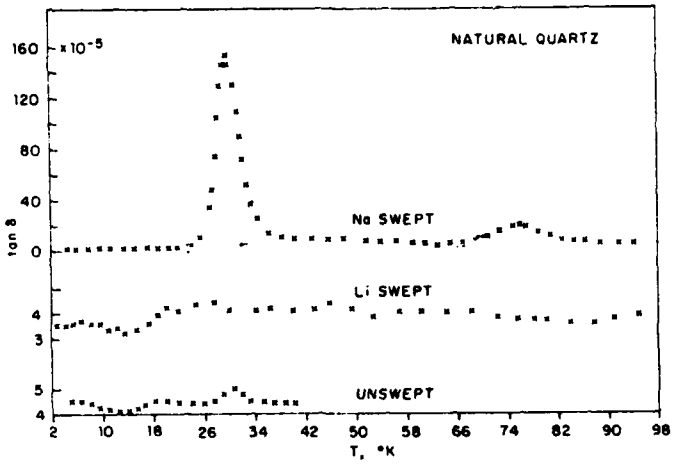

FIG. 1. Dielectric loss of natural quartz crystals that were unswept, *Li-swept* and *Na-swept*. *Note that the scale for the two lower curves* is 20 x larger than that for the upper curve.

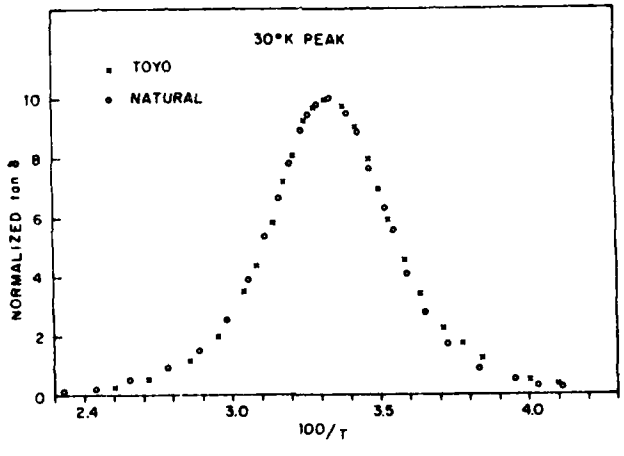

FIG. 2. The 30 K dielectric loss peak on a normalized plot for: the natural crystal, the Toyo SQ-A crystal. (The absolute peak height of the natural is 7 x higher than that of the synthetic crystal.)

The peak heights are expected to be proportional to the concentration of Al-Na pairs, and since the 30 K peak is 15 times larger than the 75 K peak it is the more sensitive indicator of Al-Na pairs. Our study of the synthetic SQ-A sample allows a calibration of the 30 K peak. Halliburton et al. [11,12] developed a method for determining the Al content of a quartz crystal by converting all of it into Al-hole ($Al\text{-}h^+$) centers through an appropriate irradiation procedure; these centers are then detected and their concentration determined through ESR measurements. In this way, they found, for an SQ-A sample from the same bar as our sample, a value of 14.4 ppm Al. If we assume that our Na-swept SQ-A sample possessed the same Al content and the Na sweeping converted all of the Al to Al-Na defect pairs, then our peak height $\tan \delta_{max} = 22.1 \times 10^{-4}$ must correspond to 14.4 ppm of Al-Na defects. This result then gives a calibration constant of 1.5×10^{-7}/ppm.

We can now use this calibration constant to obtain appropriate dipole strength. In order to do this, we need to consider the origin of the two Al-Na peaks. This question has been examined in some detail earlier [16,8]. It was deduced that the Na^+ can reside in two non-equivalent positions (say, nn and nnn) about the distorted AlO_4 tetrahedron obtained when Al^{3+} substitutes for Si^{4+} in the α-quartz structure, shown in Fig. 3. Since there is a 2-fold symmetry axis (C_2) parallel to the x-axis, each of the two Na^+ sites is matched by an equivalent site generated by the C_2 operation. Application of an electric field produces a redistribution of the Al-Na dipoles among each of the two sets of equivalent pairs. It was concluded that the lower temperature peak is due to reorientation between the two equivalent nn configurations of the pair, while the higher temperature peak is due to the nnn configurations. The magnitude of the peak, is related to the relaxation strength $\delta\varepsilon_{//}/\varepsilon_{//}$ (where $\varepsilon_{//}$ is the dielectric constant parallel to the c-axis) which is given by [17,16]

$$\delta\varepsilon_{//}/\varepsilon_{//} = 2 \tan \delta_{max} = n_d \mu_3^2 / kT \qquad (2)$$

where n_d is the number of dipoles (Al-Na pairs) per unit volume and μ_3 the component of the dipole moment parallel to the c-axis. Applying Eq.(2) to the low-temperature peak, and substituting the above calibration constant, gives $\mu_3 = 5 \times 10^{-30}$ C-m. If we simply set $\mu_3 = ex_3$, in which x_3 is the separation of charge in the c-direction, a reasonable value of $x_3 \sim 0.3$ A is obtained.

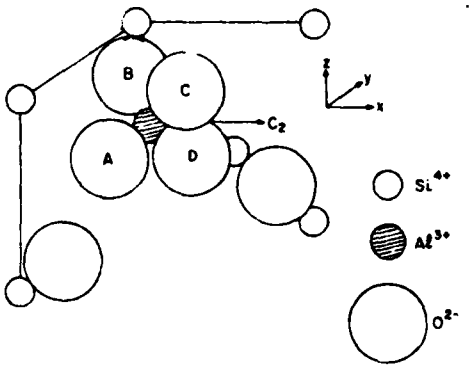

FIG. 3. Diagram showing part of the unit cell of α-quartz containing a substitutional Al^{3+} that forms an AlO_4 distorted tetrahedron. The two-fold symmetry axis, C_2, which lies parallel to the x-axis, is also shown.

Table I presents a summary of some of the results obtained for the 30 K peak for various samples. In the final column the calibration constant is used to convert peak heights into concentrations of Al-Na pairs. It is interesting that in both the natural and synthetic crystals only a very small amount of Al-Na is present in the as-grown material. In the case of high quality synthetic crystals, such as the SQ-A, grown with Li^+ in the mineralizer, this undoubtedly means that most Al^{3+} is associated with Li^+ rather than Na^+, since there is no evidence in these crystals for infrared absorption due to Al-OH centers. [18]

TABLE I. Results for the 30 K peak of various samples.

Sample	Peak Height $\tan \delta_{max} \times 10^5$	ppma Na
SQ-A unswept	3.2	2.1
SQ-A Na-swept	22.1	14.4
NQ unswept	0.8	0.5
NQ Na-swept	151	100

In view of the usefulness of the Al-Na loss peaks to monitor Na content, we have attempted to find similar peaks due to Al-Li pairs by examining several unswept and Li-swept samples cut both parallel and perpendicular to the crystal c-axis and over the entire temperature range from 2.9 to 290 K. In all of these experiments, no identifiable peak was found (in contrast to Stevels and Volger's [7] claim of a Li peak at 60 K for 32 kHz). The middle curve of Fig. 1 shows one of the best examples, that of a Li-swept natural crystal. In this case, for which the Al content is 100 ppm (see Table 1) there is no evidence for any peak as large as $\tan \delta_{max} = 1 \times 10^{-5}$. (Even small fluctuations in Fig. 1 which might hide very small peaks were later shown by remeasurement not to be peaks.) Thus, using Eq.(2), if a Al-Li peak exists for measurements parallel to the c-axis it must correspond to a value of μ_3 at least an order of magnitude smaller than for Al-Na. Similarly, measurements on perpendicularly cut crystals, for which the corresponding relaxation strength is given by [17,16]

$$\delta\epsilon_{\perp}/\epsilon_{\perp} = 2 \tan \delta_{max} = n_d \mu_2^2/2kT \qquad (3)$$

where μ_2 is the component of dipole moment in the y-direction of the crystal (see Fig. 3), is also exceedingly small. It is noteworthy that anelastic relaxation, which involves the same relaxational mode as $\epsilon_{\perp}$ [17], is also absent for Li-swept crystals over a similar temperature range. [19]

It is therefore concluded that the Al-Li pair must be oriented parallel to the x-axis, i.e. the direction of the 2-fold (C_2) symmetry axis of the crystal shown in Fig. 3. This means that the two equivalent sites between which reorientation occurs for the case of Na^+, have now collapsed into a single site, so that the possibility of reorientation under an electric field, i.e. for dielectric relaxation, no longer exists. A possible explanation for the orientation of the Al-Li pair along the C_2-axis may be related to the small size of the Li^+ ion which may permit it to sit between two oxygen ions of the AlO_4 tetrahedron. On the other hand, the Na^+ ion is believed to prefer to form an O-Na bond with one of the four oxygen ions of the tetrahedron. [8] One way to further explore these defect configurations is by computer simulations using the HADES or CASCADE-type programs. [20] Such methods have given insight into the lowest-energy configurations of different defect clusters in a variety of ionic crystals and may also be useful in the present case.

Irradiated Crystals

X-irradiation at room temperature produces a large dielectric-loss peak at very low temperatures in all of the samples studied. Figure 4 shows the results for SQ-A synthetic crystals that had been Li-, Na- and H-swept. In the Na-swept case, the 30 K (100/T = 3.3) Al-Na peak is considerably reduced and replaced by a huge peak at 8.4 K. A similar peak is present for the Li-swept case, but it is located at a lower temperature of 6.85 K. The H-swept sample, on the other hand, shows a smaller less well-defined peak after irradiation. In all cases, the dielectric loss does not decrease sharply on the low-temperature (high 1/T) side of the peak but either levels off or begins to rise gradually again.

Further information can be obtained from the effect of the measuring frequency on the peak. In most cases measurements were made at two frequencies, generally 1 kHz and 5 kHz. Figure 5 shows a typical pair of curves for the natural (NQ) Na-swept crystal, plotted as T tan δ vs. 1/T. (The choice of T tan δ is made based on Eq.(2) which shows that tan δ varies inversely as T.) The figure shows the usual shift to higher peak temperature with higher frequency, but also that tan δ decreases much more sharply on the low-temperature side at 5 kHz than at 1 kHz. This behavior strongly suggests that the low-temperature shelf in the data of Fig. 4 at 1 kHz is not an additional background effect, but arises because the relaxation time does not continue to obey the Arrhenius equation (1) down to the lowest temperatures. Such behavior is to be expected when quantum effects, e.g. quantum-mechanical tunneling, set in at low temperatures, so that τ varies only slowly with T in that range. This conclusion was also suggested by de Vos and Volger [21] from their studies of dielectric loss in natural smoky quartz crystals, where they measured the relaxation peak as a function of frequency at a series of fixed temperatures. Figure 5 also shows that the irradiation peak is much larger in the natural crystal than in the synthetic, consistent with the much higher Al content of the natural crystal. It is also interesting that the peak temperature is higher for the NQ than for the SQ-A Na-swept samples, i.e. the peak temperature is dependent on the total Al-M^+ impurity content.

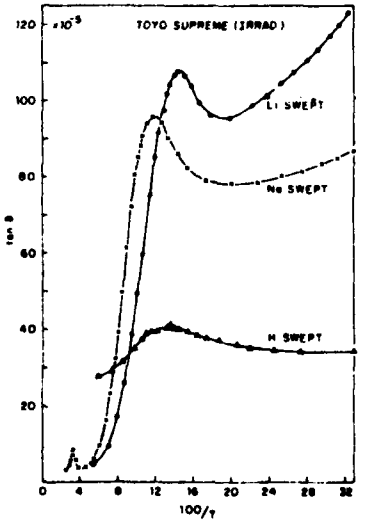

FIG. 4. Dielectric loss of three differently swept synthetic SQ-A samples following X-irradiation.

In order to obtain the dependence of the relaxation time τ on temperature over the range of the peak, the following method of analysis was used. The peak was expressed in the Fuoss-Kirkwood form [15]

$$T \tan \delta = A \operatorname{sech} \alpha x \qquad (4)$$

where $A = (T \tan \delta)_{max}$, $x = \ln \omega\tau$ and $\alpha (\leq 1)$ is a parameter that determines the width of the distribution, a Debye peak having the value $\alpha = 1$. Data for two different frequencies were utilized, and it was required that $\tau(T)$ from both sets of data come out the same. With the aid of a computer program, $\alpha(T)$ is calculated from this requirement and then $\tau(T)$ is obtained. The values of α fall in the range 0.6 to 0.8. The curves of $\tau(T)$ so generated are shown in Fig. 6 for Li- and Na-swept SO-A synthetic samples. Each curve shows an Arrhenius range at the higher temperatures and a quantum range at low temperatures. In this sense, there is agreement with de Vos and Volger [20] who also found two such stages. The activation energies, obtained from the Arrhenius range in Fig. 6 are 5.1 and 7.5 meV, respectively for the Li- and Na-swept samples. The corresponding τ_0 values are $1.5 \times 10^{-}$ and $5.6 \times 10^{}$ sec^{-1}. The low temperature range shows $\tau \propto 1/T$, which is indicative of phonon-assisted tunneling.

Annealing experiments were also carried out. The low-temperature irradiation peak anneals out in the range between 450 and 550 K, as shown in Fig. 7. For the Na-swept samples, the Al-Na peak is restored as the irradiation peak decreases. It is striking that the annealing curves for the Li-swept (or unswept, which contains mostly Li) and Na-swept samples are different, with the Na-swept sample annealing at higher temperatures and in a narrower temperature range than the Li-swept.

The question of the origin of these low-temperature irradiation peaks is a most interesting one. Clearly the peak height is related to the total Al content (compare, e.g. SQ-A and NQ samples) and is more prominent when alkalis are present than H^+ (see H-swept in Fig. 4). If either all of the Al or the alkali present is involved in this peak, the corresponding dipole moment μ_j [see Eq.(2)] obtained is ~ 5 times greater than that for the Al-Na peak. The low pre-exponential value in the Arrhenius range as well as the onset of quantum-mechanical tunneling at the lowest temperatures suggest that an electronic defect is involved in the relaxation. The aluminum-hole, Al-h^+,

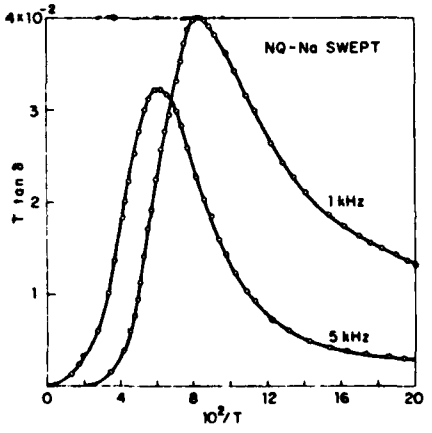

FIG. 5. Plot of T tan δ versus 1/T for a natural (NQ) Na-swept crystal after irradiation, as measured at 1 and 5 kHz.

center which is present after irradiation and gives rise to a well known ESR spectrum [11], has been suggested as the source of this peak, [21] Objections to this suggestion, however, are the fact that the peak is different for Na- and Li-swept crytals (Fig. 4), and that annealing of the Al-h^+ center as measured directly by ESR, appears to occur at somewhat higher temperatures [12] than observed here. Alternatively, we may consider alkali (M^+) centers. A simple alakli-electron center ($M-e^-$) is not likely since such a center would have a well defined ESR spectrum, which has not been observed in irradiated samples. [22] A more complex alkali center may be involved, however. For example, it may contain two electrons and possibly an oxygen-ion vacancy. The possibility that these dielectric loss peaks originate in an alkali center is of great interest, since there has been no evidence from other techniques to indicate what becomes of the alkali ion after it is liberated from a Al-M^+ pair by irradiation. Further work is required, however, before the origin of these interesting radiation induced dielectric-loss peaks can definitely be established.

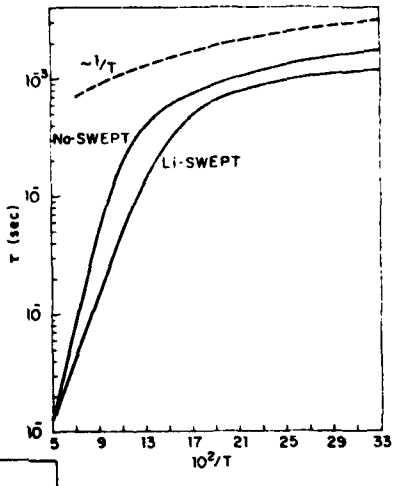

FIG. 6. Comparison of log τ vs. 1/T plots for Na-swept and Li-swept synthetic SQ-A samples, calculated from the irradiation-induced dielectric loss peaks as described in the text. The dashed line represents $\tau \sim 1/T$.

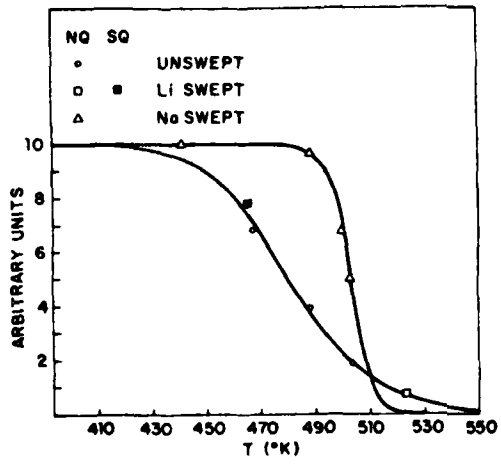

FIG. 7. Isochronal annealing curves of irradiation-induced dielectric loss peaks for Li-swept and Na-swept natural (NQ) crystals. The ordinate plots the relative peak height, and the anneal time is 15 min.

ACKNOWLEDGEMENTS

The authors are grateful to Prof. Joel Martin for carrying out electrodiffusion on the samples studied here, and to Prof. L. Halliburton for helpful suggestions. This work was supported by the U.S. Air Force under contract F 19628-82-K-0013.

REFERENCES

1. See, e.g., Proc. 37th Annual Symp. on Freq. Control, U.S. AFRADCOM, Ft. Monmouth, N.J. and IEEE, 1983.
2. J.C. King and H.H. Sander, Radiation Effects 26 (1975) 203.
3. D.R. Koehler and J.J. Martin, ref. 1, p. 130.
4. A. Kats, Philips Res. Rep. 17 (1962) 133.
5. R.N. Brown and A. Kahan, J. Phys. Chem. Solids 36 (1975) 467.
6. W.A. Sibley, J.J. Martin, M.C. Wintersgill and J.D. Brown, J. Appl. Phys. 50 (1979) 5449.
7. J.M. Stevels and J. Volger, Philips Res. Rep. 17 (1962) 283.
8. D.S. Park and A.S. Nowick, Phys. Stat. Sol. (a) 26 (1974) 617.
9. D.B. Fraser, in: Physical Acoustics, Vol. V, ed. W.P. Mason (Academic Press, New York, 1968), Chap. 2.
10. H. Jain and A.S. Nowick, J. Appl. Phys. 53 (1982) 477.
11. M.E. Markes and L.E. Halliburton, J. Appl. Phys. 50 (1979) 8172.
12. L.E. Halliburton, N. Koumvakalis, M.E. Markes and J.J. Martin, J. Appl. Phys. 52 (1981) 3565.
13. J.C. King, Bell Syst. Tech. J. 38 (1959) 573.
14. S.P. Dougherty, J.J. Martin, H.F. Armington and R.N. Brown, J. Appl. Phys. 51 (1980) 4164.
15. A.S. Nowick and B.S. Berry, Anelastic Relaxation in Crystalline Solids (Academic Press, New York, 1972), Chapters 3-4.
16. A.S. Nowick and M.W. Stanley, in: Physics of the Solid State, ed. S. Balakrishna (Academic Press, New York, 1969), p. 183.
17. A.S. Nowick and W.R. Heller, Adv. Phys. 14 (1965) 101.
18. J.J. Martin, private communication.
19. J.J. Martin, L.E. Halliburton and R.B. Bossoli, Proc. 35th Annual Symp. Freq. Control, U.S. AERADCOM, 1981, p. 317.
20. W.C. Mackrodt, in: Computer Simulation of Solids, ed. C.R.A. Catlow and W.C. Mackrodt (Springer-Verlag, Berlin, 1982), Chapter 12.
21. W.J. deVos and J. Volger, Physica 34 (1967) 272; 47 (1970) 13.
22. L.E. Halliburton, private communication.

EFFECT OF IRRADIATION AND ANNEALING ON THE ELECTRICAL CONDUCTIVITY OF QUARTZ CRYSTALS

E.R. Green, J. Toulouse, J. Wacks and A.S. Nowick
Krumb School of Mines, Columbia University
New York, N.Y. 10027

Summary

In order to better understand the defects produced in α-quartz by irradiation, electrical conductivity measurements provide a valuable tool. A detailed study was made of the radiation-induced conductivity (RIC) of a variety of crystals, including both cultured and natural crystals that had been either Li- or Na-swept. X-ray irradiation was carried out at and below room temperature (from 150-300 K) and subsequent annealing up to ∿ 450° C. Immediately after low-temperature irradiation the RIC showed an activation energy, E, of 0.28 ± 0.02 eV. With annealing E increased and the RIC decreased. Irradiation at 150 K gave a larger RIC than irradiations above 200 K, where alkalis M^+ are known to be released from Al-M^+ pairs. Isochronal annealing to elevated temperatures showed an overshoot phenomenon, whereby the conductivity fell to values below those of the unirradiated crystal, after which it annealed upwards.

Consideration of the principal results of these experiments led to the conclusion that the RIC is most readily explained in terms of electronic rather than ionic defects, viz., polaron-like holes that have a hopping activation energy of 0.28 eV. There remain questions to be answered, however, before this mechanism can be regarded as definitely established.

Introduction

The effects of radiation on the frequency of quartz-crystal resonators is well known.[1-3] Radiation induced changes in frequency are related to changes in defect structures induced by the radiation. Of central importance in this regard is the Al-M^+ defect, where Al denotes an Al^{3+} ion substituting for Si^{4+}, and M^+ an alkali (primarily Li^+ or Na^+) located in an adjacent interstitial position. The Al-Na^+ center can be detected through a characteristic pair of anelastic loss peaks[4] as well as by a pair of dielectric loss peaks.[5,6] There are no comparable Al-Li^+ peaks, however.[7] It has been shown[8,9] that irradiation at temperatures above 200 K liberates the alkali from the Al-M^+ pair, replacing it either with a hole h^+ or a proton H^+ which binds to a nearby oxygen ion to form an OH^- ion. The corresponding Al-h^+ defect is directly observable by means of electron spin resonance (ESR) measurements[10] while the Al-OH center is observable through characteristic infrared (IR) absorption bands.[11,9] Thus, techniques are available for the study of the formation and annealing of these two centers. On the other hand, our ability to follow the course of the alkalis subsequent to their liberation from Al-M^+ centers by irradiation has been very limited. Radiation induced dielectric peaks at very low temperatures have been studied which appear to be due to alkali centers,[12] but the details concerning such peaks are not yet fully sorted out. Yet there is considerable evidence that radiation-induced frequency changes are greatly influenced by defects involving the alkalis.

An opportunity to follow the alkalis subsequently to irradiation is offered by electrical conductivity measurements. It is well known that the conductivity of unirradiated α-quartz crystals is ionic in origin and that the carriers are M^+ ions liberated from Al-M^+ pairs, which then migrate preferentially along the open c-axis channels of the crystal structure.[13] Radiation-induced conductivity (RIC) has also been studied. Here it was shown (using a pulse irradiation source) that there are two effects: one at very short times (∿ msec) which has been attributed to electronic defects, and the second at longer times which has been attributed to M^+ ions freed from Al-M^+ centers.[4] A strong argument that the longer term RIC is due to M^+ ions is the high anisotropy of the effect, viz. the fact that the conductivity parallel to the c-axis is much larger than that perpendicular to the c-axis, suggesting the migration of interstitial ions in the open channels.[14,15]

The present work is a further and more detailed study of the long-term RIC and of the effects of annealing after irradiation. Most of the crystals studied were electrodiffused ("swept") so that the alkali present was essentially either all Li^+ or all Na^+. X-ray irradiation was carried out at and below room temperature, and the effects on conductivity immediately following the irradiation and after step annealing up to temperatures ∿ 450° C will be reported. The work leads to conclusions that were initially quite unexpected.

Theory of the Conductivity

This section will review some of the basic equations that describe the conductivity and will be required for later reference.

If the conductivity, σ, is dominated by one carrier, e.g. the alkali ion, M^+, it can be expressed as

$$\sigma = x_c N_o e \mu_c \qquad (1)$$

where x_c is the mole fraction of the carriers, N_o the number of SiO_2 molecules per unit volume, e the charge on the carrier and μ_c its mobility. It is the quantity μ_c that can be highly anisotropic in the crystal of α-quartz. Except where otherwise stated, in this paper μ_c and σ will both refer to the direction parallel to the c-axis. In general both x_c and μ_c are temperature dependent. The mobility is given by

$$\mu_c = ed^2 w_c / kT \qquad (2)$$

where d is the component of jump distance parallel to the c-axis, kT has the usual meaning, and w_c is the jump frequency of the carrier defect, given by

$$w_c = \nu_0' \exp(-E_m/kT) \quad (3)$$

Here ν_0' (usually $\sim 10^{13}$ sec^{-1}) includes both the attempt frequency and an entropy factor for the migrating defect, while E_m is the motional activation energy.

For the quantity x_c there are two important cases. Under equilibrium conditions, with most of the M^+ carriers associated as Al-M^+ pairs, the value of x_c is obtained from the mass action relation for the association equilibrium, and takes the form:

$$x_c \propto \exp(-mE_A/kT) \quad (4)$$

where E_A is the association energy of the pair and m = ½ or 1 depending on the detailed situation involving other defects.[13] Thus, combining eqs. (1)-(4), in the lower temperature range (where association is nearly complete), σ obeys the Arrhenius-type relation

$$\sigma T = A \exp(-E/kT) \quad (5)$$

in which the "conductivity activation energy" E is given by

$$E = E_m + mE_A \quad (6)$$

The preexponential factor A can also be explicitly evaluated.

The second relatively simple case for x_c is the nonequilibrium one, where, immediately after irradiation x_c is frozen in at a constant value, independent of temperature. This applies so long as the temperature is kept low enough to avoid annealing. In this case, we again obtain Eq. (5), but now

$$E = E_m \quad (7)$$

and

$$A = x_c N_\sigma d^2 e^2 \nu_0'/k \quad (8)$$

Since all other constants are reasonably well known, Eq. (8) may be used to calculate x_c from the experimental value of the preexponential factor A.

Methods

The principal cultured crystals studied were high quality crystals taken from the Z-growth region: Toyo Supreme Q (bar SQ-A), Sawyer Premium Q (bar PQ-E) and High aluminum grown in the Soviet Union (bar HA-A). The natural crystal (NQ) was a clear crystal from Arkansas.

Electrodiffusion experiments were carried out at Oklahoma State University by Dr. J. Martin.[16] These included Li^+ sweeping, Na^+ sweeping and, in one case, H^+ sweeping.

X-ray irradiation was carried out for a period of 2 to 4 hours using a conventional tungsten-filament tube at 40 kV and 20 mA. The dose was $\sim 3\times10^6$ R. The very soft X-rays were filtered out by the layer of sputtered silver used as electrodes.

For irradiation below room temperature a special cell was built to make it possible to carry out conductivity measurements without warm-up. The cell was cooled with a dry-ice/ethanol mixture and with liquid nitrogen for still lower temperatures. With the aid of a heating coil it was possible to achieve the temperature range from 150 - 400 K in this apparatus. For the higher temperature measurements the sample was placed in a standard conductivity cell which could go up to 500° C.

Conductivity measurements were made with a General Radio type 1620A Capacitance Bridge assembly over the frequency range 20 Hz - 100 kHz. In most cases, complex impedance analysis was used to obtain the bulk conductance.[13] The samples were plates of surface area 1 cm^2 and thickness 1.0 - 1.5 mm coated with sputtered silver electrodes.

Results

Unirradiated Crystals

A listing of the samples studied and the best estimates of their Al contents is given in Table I. (In most cases the Al content was obtained from the peak height of the principal Al-Na dielectric loss peak in the Na swept material; in some cases the strength of the Al-h^+ ESR signal after the irradiation sequences of Markes and Halliburton[6] was used). Arrhenius plots of the conductivity are given in Fig. 1. At the lower temperatures all of these plots give good straight lines. Table II lists the activation energies, E, and preexponentials, A, obtained from these straight line portions. The results show that differences in σ between Li-swept and Na-swept samples from the same stone are small, generally well within an order of magnitude. Except for the HA-A samples, $\sigma_{Li} > \sigma_{Na}$; however E_{Li} is slightly greater than E_{Na} for all of the cultured crystals. It should be recalled that E is made up of terms related both to the motion and the association energy of the carrier [Eq. (6)]. The significance of these results and of the corresponding preexponentials, A, will be discussed elsewhere.[17]

The two lowest curves of Fig. 1 are especially interesting. The second lowest is the SQ-A H-swept sample (i.e. air swept). It shows that substituting H^+ for alkalis lowers σ by two orders of magnitude, yet keeps E unchanged. This strongly suggests that residual alkalis are still the carriers, and that H^+ is far less mobile than alkali ions.

Table I. Crystals Studied.

Name	Type	Al(ppma)
NQ	Natural	69
SQ-A	Cultured (Toyo)	13
PQ-E	Cultured (Sawyer)	15
HA-A	Cultured (Russian)	355
GEC	Cultured (GEC Ltd)	<0.1

The lowest curve is that for the highest purity (GEC) sample[18] and indicates that here too, σ is suppressed because of the very low alkali content. The similarity between this curve and that of the H-swept SQ-A sample in Fig. 1 is quite striking.

Irradiated Crystals: Low Temperatures

With the apparatus described earlier, it has been

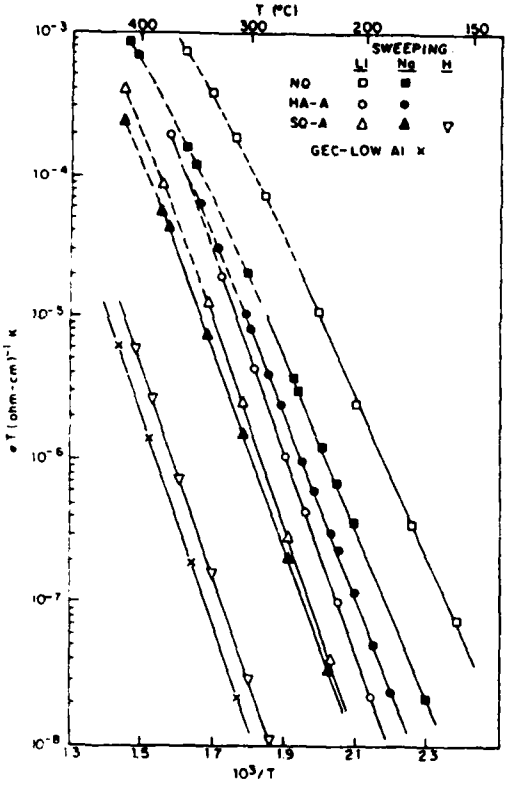

Fig. 1. Arrhenius plots of the conductivity (log σT vs. T^{-1}) for various unirradiated samples.

possible to carry out irradiations below room temperature and then to begin measurements immediately in situ. Three different sets of samples were investigated in this manner: HA-A and NQ (both Li and Na-swept), and PQ-E (Li-swept only). Figure 2 shows results for NQ-Li after irradiation at 210 K. Curve (a) is the initial run (up to -29° C); then after several additional runs in this temperature range (not shown), curve (b) was

Table II. Summary of Results on Conductivity of Unirradiated Samples.

Sample	E(eV)	$A(\Omega^{-1}cm^{-1}K)$
NQ-Li	1.11	1.4×10^6
NQ-Na	1.19	1.2×10^6
HA-A-Li	1.38	1.9×10^7
HA-A-Na	1.32	1.6×10^7
SQ-A-Li	1.43	1.5×10^7
SQ-A-Na	1.36	2.2×10^6
SQ-A-H	1.42	2.3×10^5
GEC-Low Al	1.42	1.4×10^5

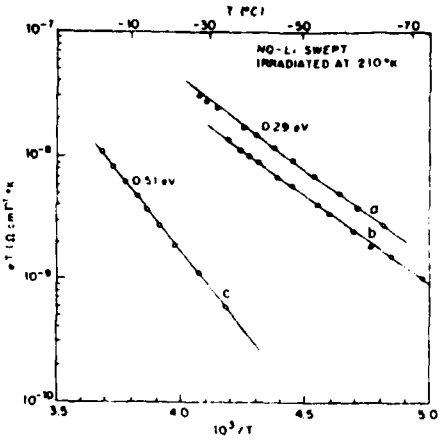

Fig. 2. Conductivity plots of an NQ-Li swept sample irradiated at 210 K: a) immediately after irradiation, b) after several runs below -29° C, and c) after a ½h anneal at 4° C.

obtained, showing that only a small amount of annealing and virtually no change in activation energy (E = 0.29 eV) have occurred. After ½h at 4° C curve (c) is obtained, showing considerable annealing and an appreciable increase in E.

It is noteworthy that σ in curve (a), say at 220 K, is 10^{11} times higher than the value extrapolated from Fig. 1 for the same crystal. In this sense, then, the effect of irradiation is truly spectacular. For the same irradiation, high quality cultured crystals, such as SQ-A and PQ-E give initial conductivities almost an order of magnitude lower than that for the natural crystal, NQ, but of course still enormously greater than the equilibrium values.

Figure 3 shows the effect of irradiation temperature, showing initial runs on a PQ-E-Li swept sample after two different irradiations, one at 150 K and the other at 240 K. It is striking that the conductivity after 150 K irradiation is so high even though the irradiation temperature lies below the range in which alkalis are liberated from Al-M^+ centers.[8,9] Table III summarizes the results for the various as-irradiated samples showing the values of E and A obtained as well as the conductivity at -51° C (1000/T = 4.5). It is interesting that the initial activation energies fall within a narrow range of 0.28 ± 0.02 eV except for the sample irradiated at the highest temperature (240 K). The final column of Table III is the value of x_c calculated from Eq. (8) and the measured value of A, under the assumption that $E=E_m$ (i.e. x_c is a constant).

As annealing after irradiation is continued at higher and higher temperatures or for long time periods, σ continues to decrease and E to increase, in the manner already shown in Fig. 2. Further annealing studies were carried out in the range above room temperature.

Irradiated Crystals: Elevated Temperatures

For the study of behavior of irradiated samples well above room temperature, there seemed to be no need to irradiate below room temperature. Therefore, for convenience, room temperature irradiations were used. As already indicated, considerable annealing of the conductivity takes place as irradiated crystals are warmed up. Figure 4 shows a series of isothermal

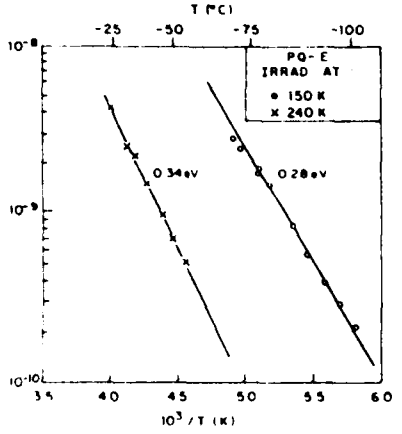

Fig. 3. Conductivity plots of a PQ-E-Li swept sample immediately after irradiation at two different temperatures: 150 K and 240 K.

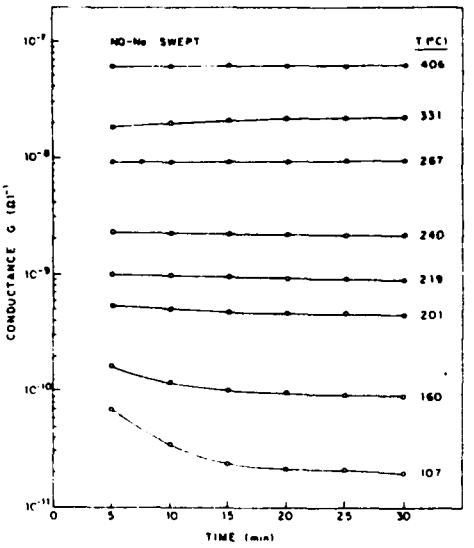

Fig. 4. Isothermal annealing curves carried out at successively increasing temperatures for NQ-Na swept sample after room temperature irradiation.

annealing curves carried out at successively increasing temperatures. It shows a surprising reversal of the direction of annealing. Thus, while σ decreased with time at temperatures up to 219° C, it remained almost constant at 240° and 267° C, then started to increase isothermally at 331° and higher. It is helpful to plot the data isochronally, as in Fig. 5. Here we plot log σT versus 1/T in the usual way, but comparing the equilibrium data of Fig. 1 with values obtained after 1h anneal at successively increasing temperatures. The SQ-A cultured and the natural NQ samples, both Li swept, are shown. The cross-over or "overshoot" effect demonstrated in Fig. 5 has been observed for all of the alkali swept samples studied after irradiation. Note that the conductivity finally returns to the equilibrium curve only after anneals at ≈ 450° C.

It is illuminating to represent the annealing data as a plot of Δ ln σ versus temperature, where

$$\Delta \ln \sigma \equiv \ln (\sigma_{irr}/\sigma_{unirr}) \qquad (9)$$

Here σ_{irr} is the conductivity of the irradiated and isochronally annealed sample while σ_{unirr} is that of the unirradiated sample. Thus Δ ln σ is the difference in ordinates between the irradiated and unirradiated curves in Fig. 5. Δ ln σ = 0 represents the cross-over of the two curves, while negative values represent the range in which the irradiated curve falls below the unirradiated. Figure 6 shows such a plot for the NQ-Na swept and the NQ-Li swept samples. It is interesting that the Li-swept case crosses over sooner than the Na-swept. A similar plot for the cultured SQ-A-Na crystal

Table III. Summary of Results on Conductivity of As-Irradiated Samples. [x_c is the mole fraction of carriers calculated from Eq. (8)].

Sample	Irrad. Temp. (°K)	σT at -51° C	E (eV)	A(Ω⁻¹cm⁻¹K)	x_c(ppm)
NQ-Na	210	3×10^{-9}	0.27	4.6×10^{-3}	3×10^{-2}
NQ-Li	210	8×10^{-9}	0.29	2.9×10^{-2}	1.8×10^{-1}
HA-A-Na	215	7×10^{-11}	0.26	4.3×10^{-5}	3×10^{-4}
HA-A-Li	210	3×10^{-11}	0.30	2.1×10^{-4}	1.4×10^{-3}
PQ-E-Li	150	1.2×10^{-8}	0.28	2.9×10^{-2}	1.8×10^{-1}
PQ-E-Li	240	6×10^{-10}	0.34	3.2×10^{-2}	2×10^{-1}

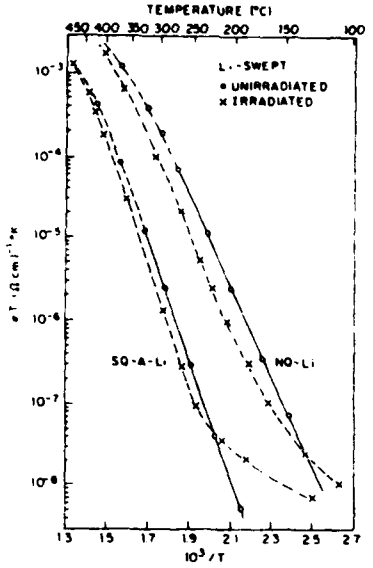

Fig. 5. Conductivity plots comparing unirradiated sample (circles) to isochronally ($\frac{1}{2}$h) annealed sample at successively increasing temperatures following room temperature irradiation (crosses). Data are for NQ and SQ-A samples, both Li-swept.

is shown in Fig. 7. In this case we have also marked the annealing stages observed by others on similar samples, using ESR, IR and anelastic relaxation methods.[19] Stage I is the region in which Al-OH centers increase, apparently without comparable changes in the other observable centers. Stage II is the well defined annealing stage in which the Al-h^+ center anneals out with a partial recovery of Al-Na^+. Finally, in stage III the Al-OH centers disappear and are replaced by Al-Na, which now account for all of the Al centers, as before irradiation.

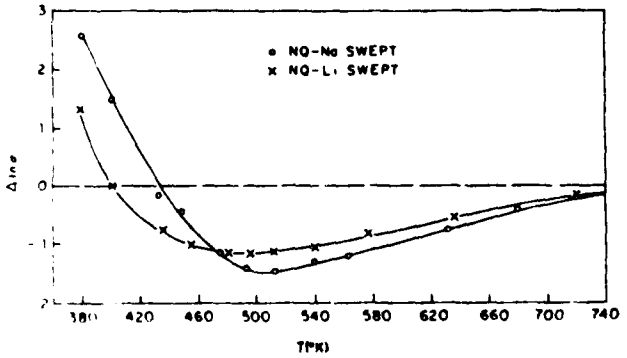

Fig. 6. Isochronal plot of Δ ln σ versus temperature for two samples: NQ-Na and NQ-Li swept. Δ ln σ is defined by Eq. (9).

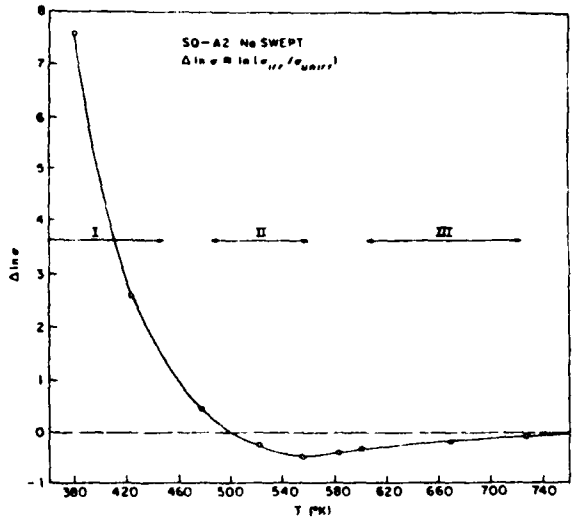

Fig. 7. Isochronal plot similar to Fig. 6 for SQ-A, Na swept sample. Also shown are the temperature ranges of three annealing stages previously reported.[19]

The comparison of these stages with the present annealing curve is somewhat inexact because of differences in the type of irradiation and the samples employed by ourselves and the other investigators. A more exact comparison has been made in this laboratory between the conductivity annealing of the NQ-Na and NQ-Li samples of Fig. 6 and the annealing out of the low temperature dielectric peak produced by irradiation.[12] While this dielectric peak has been attributed to alkali centers rather than to Al-h^+, we have recently shown that it anneals almost precisely together with the Al-h^+ center, i.e. in Stage II.[17] Comparison of the annealing curves of the low temperature dielectric peak[12] with the data of Fig. 5 shows that it anneals precisely in the range in which Δ ln σ is close to its minimum value. In other words, the Δ ln σ curves are essentially quiescent when the important Stage II annealing process is taking place. This observation will be of special significance to the discussion of the next section.

Discussion

It has been customary to regard the long-term radiation-induced conductivity (RIC) as due to ionic (alkali ion) carriers, that are considerably enhanced in their numbers by the irradiation. The principal argument for this viewpoint is the high anisotropy of the long-time RIC, favoring the direction parallel to the crystal c-axis.[14,15] This anisotropy is more consistent with freed alkali ions running along c-axis channels than with electrons and/or holes in energy bands of the crystal. The present work, however, has yielded a number of key facts that are difficult to explain by the ionic mechanism. These facts may be summarized as follows:

1) The magnitude of the RIC immediately after irradiation is not diminished, but is in fact increased, when irradiation is carried out below 200 K (where other experiments have demonstrated that alkali ions are not liberated from Al-M^+ centers).[8,9] See Fig. 3.

2) The magnitude of the RIC is smallest for the cultured crystal (HA-A) that has the highest Al content. See Table III.

3) Immediately after low temperature irradiation an activation energy E = 0.28±0.02 eV is found for both Li-and Na-swept samples (although the value for Na is perhaps consistently slightly lower than that for Li). See Table III.

4) Upon annealing, the conductivity shows the overshoot phenomenon, falling to values below that of the unirradiated crystal. See Fig. 5.

5) The important annealing Stage II (where Al-h^+ centers, as well as the low-temperature dielectric peak attributed to alkali centers, disappear) takes place in a range in which $\Delta \ln \sigma$ is not changing. See Fig. 6.

As already mentioned, these facts do not absolutely rule out an ionic mechanism, but one must invoke complexities that strain the model, e.g. the existence of a variety of ill-defined deep traps of different depths for the alkalis. We will not attempt to develop such a model in this paper.

On the other hand, if we were to postulate an electronic model, specifically claiming that low-mobility electron holes dominate the long-term conductivity after irradiation, then most of the above mentioned facts can be readily explained. It is then reasonable to suppose that the minimum in the $\Delta \ln \sigma$ curves (Figs. 6 and 7) represents the point in which the dominance of hole conductivity ceases and ionic conductivity begins to take over. The minimum is not then a point of zero change, where the concentration of carriers remains constant, but merely the sum of a sharply decreasing curve for the conductivity contributed by holes and an increasing curve for that contributed by alkalis. Item 5 above is then no longer a problem. As for items 1 and 2, for hole dominated RIC, the largest conductivities should indeed arise when the fewest Al-h^+ centers are produced, viz., when T is below 200 K or when the Al content is relatively low.

In terms of this interpretation, the holes must be self trapped by the lattice relaxations and therefore move as polarons. The initial activation energy of 0.28 eV would then represent the activation energy for migration of these holes and, of course, the same value should then be obtained for Li- as for Na-swept crystals (item 3). The values of x_c in the last column of Table III then represent the concentration of such holes. Note the extremely small value for these freely migrating defects (10^{-4} to 10^{-1} ppm).

Two questions then arise. First, is there any other evidence for such defects in quartz? A possible "yes" answer comes from work on ultraviolet photoelectron spectroscopy in amorphous SiO_2, which makes it possible to probe the structure of the valence band.[20] A narrow nonbonding orbital subband is found near the valence-band edge indicating low hole mobility with possible lattice trapping of these holes. It is also indicated that the valence-band structure of crystalline α-quartz should be similar. The second question is whether such polaron-like holes could migrate preferentially along the c-axis, in order to account for the large anisotropy. This question is unanswered at present.

Further experiments to demonstrate more directly whether the RIC is electronic in origin are desirable. Nevertheless, at this stage, the explanation of the present experiments in terms of electronic defects seems to provide the most reasonable interpretation for the observations reported herein, and a new viewpoint concerning radiation-induced conductivity.

Acknowledgements

The authors are grateful to Prof. Joel Martin for carrying out electrodiffusion on the various samples studied here. This work was supported by the U.S. Air Force under contract F 19628-82-K-0013 and monitored by H.G. Lipson, RADC Hanscom AFB.

References

1. J.C. King and H.H. Sander, Rad. Effects 26, 203 (1975).
2. B.R. Capone, A. Kahan, R.N. Brown and J.R. Buckmelter, IEE Trans. on Nucl. Sci. NS-13, 130 (1966).
3. H.G. Lipson, F. Euler and P.A. Ligor, Proc. 33rd Ann. Freq. Control Symp., USAERADCOM, Ft. Monmouth, N.J., p. 122 (1979).
4. D.B. Fraser, in Physical Acoustics, Vol. V, W.P. Mason, editor, Academic Press, N.Y., 1968, Chapter 2.
5. J.M. Stevels and J. Volger, Philips Res. Rep. 17, 283 (1962).
6. D.S. Park and A.S. Nowick, Phys. Stat. Sol. (a) 26, 617 (1974).
7. J. Toulouse, E.R. Green and A.S. Nowick, Proc. 37th Ann. Freq. Control Symp., USAERADCOM, p. 125, (1983).
8. S.P. Dougherty, J.J. Martin, A.F. Armington and R.N. Brown, J. Appl. Phys. 51, 4164 (1980).
9. L.E. Halliburton, N. Koumvakalis, M.E. Markes and J.J. Martin, J. Appl. Phys. 52, 3565 (1981).
10. M.E. Markes and L.E. Halliburton, J. Appl. Phys. 50, 8172 (1979).
11. H.G. Lipson, F. Euler and A.F. Armington, Proc. 32nd Ann. Freq. Control Symp., USAERADCOM, p. 11 (1978).
12. J. Toulouse and A.S. Nowick, Proc. Symp. on Defect Properties and Processing of High-Technology Nonmetallic Materials. In press, 1984.
13. H. Jain and A.S. Nowick, J. Appl. Phys. 53, 477 (1982).
14. R.C. Hughes, Rad. Effects 26, 225 (1975).
15. H. Jain and A.S. Nowick, J. Appl. Phys. 53, 485 (1982).
16. J.J. Martin, R.B. Bossoli and L.E. Halliburton, Proc. 37th Ann. Freq. Control Symp., USAERADCOM, p. 164 (1983).
17. J. Toulouse and A.S. Nowick, to be published.
18. S.P. Dougherty, S.E. Morris, D.C. Andrews and D.F. Croxall, Proc. 36th Ann. Freq. Control Symp., USAERADCOM, p. 66 (1982).
19. J.J. Martin, this Symposium.
20. T.H. DiStefano and D.E. Eastman, Phys. Rev. Lett. 27, 1560 (1971).

SOME TECHNIQUES FOR THE STUDY OF ATOMIC MOTIONS WITH APPLICATIONS TO CERAMIC MATERIALS

A.S. Nowick

Henry Krumb School of Mines
Columbia University, New York, N.Y. 10027, USA

ABSTRACT

A review is presented of the use of the techniques of a.c. impedance measurements, dielectric relaxation and anelastic relaxation to study technologically interesting ceramic materials. Illustrations are given of the application of these methods to the study of solid electrolytes as well as quartz crystals used for frequency control.

INTRODUCTION

Knowledge of rates of atom movements plays an important role in the understanding of most materials. In the case of ceramic (ionic) materials, the migrating species are often charged ions, and then their migration rates can be studied by electrical means. Such studies are of particular interest in the case of materials that are relatively good ionic conductors, the so-called solid electrolytes or "superionic conductors" which are of interest as electrolytes for solid-state batteries and fuel cells. Such applications are of sufficient interest that in recent years there has been an outpouring of review books [1-3] and conference proceedings [4-7] in this area. Materials studied include those that conduct by migration of alkali ions, silver ions, protons, oxygen ions and fluorine ions, among others.

The present paper will review three techniques that have been actively used in recent years in the author's laboratory, with illustrations of the kind of information, both basic and applied, derivable from them. The techniques are: (1) a.c. impedance measurement, (2) dielectric relaxation, and (3) anelastic relaxation. We will see that valuable information about technologically important systems has been obtained using these techniques.

A.C. IMPEDANCE MEASUREMENT AND ANALYSIS

An ideal ionically conducting material should be represented electrically as a capacitance C in parallel with a resistance R, the former representing the dielectric properties of the medium and the latter its conduction. Real materials are not so simple, however, due to a number of complications. First, there is the problem of introducing and discharging the conducting ionic species at the respective electrodes. Second, one finds another effect, loosely called the "grain-boundary" effect, which is due to blocking of carriers at internal interfaces within the electrolyte. As a result of these factors the actual equivalent circuit of a sample can be extremely complex. A relatively simple representation is shown in

Fig. 1a, consisting of three R-C units in series with each other, one representing the bulk or lattice behavior, another the grain-boundary effect and the final one, the electrode effect. In order to study such an equivalent circuit, a.c. measurements are made over as wide a frequency range ("frequency window") as possible (usually 1 Hz to 10^6 Hz). The sample can then be represented by its complex admittance, Y* containing both real and imaginary parts (representing the current in-phase with and 90^0 out-of-phase with the applied voltage). One may write

$$Y^* = G(\omega) + i\omega C(\omega) \qquad (1)$$

where $G(\omega)$ is the effective conductance and $C(\omega)$ the capacitance both, in general, functions of the frequency. We may also introduce the reciprocal quantity, $Z^* = 1/Y^*$, called the complex impedance, which also has real and imaginary parts

$$Z^* = Z'(\omega) - iZ''(\omega) \qquad (2)$$

A convenient and widely used analysis is the complex impedance plot in which Z" is plotted as a function of Z' with ω as parameter. For the case of the equivalent circuit shown in Fig. 1a, such a plot yields three semicircular arcs, one for each R-C unit, as shown in Fig. 1b. In this plot the frequency increases as we go from right to left (arc 1 to arc 3). In this way, it becomes possible to separate out the true lattice conduction from the grain-boundary and electrode phenomena, and to study each separately.

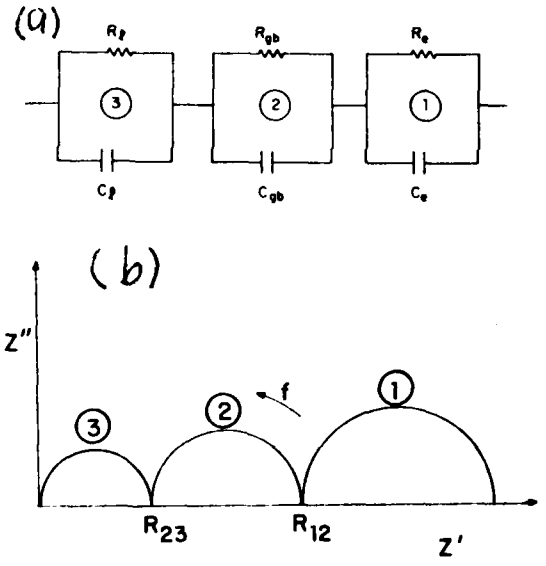

Fig. 1a. Equivalent circuit representing lattice (ℓ), grain boundary (gb) and electrode (e) effects.

Fig. 1b. Schematic diagram of complex impedance plot corresponding to circuit of part (a). Arrow indicates direction of increasing frequency.

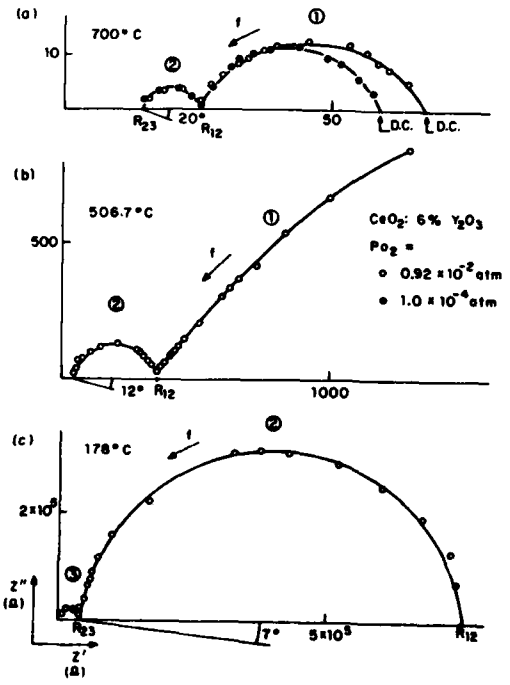

Fig. 2. Examples of complex impedance plots for CeO_2:6% Y_2O_3 at three different temperatures. Arcs are labeled to match Fig. 1b. From Ref. [8].

Actually, the experimental "frequency window" is usually not wide enough to display all three effects at any one temperature, but by covering a range of temperatures, we can see all of them. Figure 2 shows an example for the case of Y^{3+} doped CeO_2. This material is an oxygen-ion conductor through the migration of oxygen-ion vacancies which are introduced into the lattice as charge compensation for the lower valent cation dopant. Such ionic conductors may be used as the solid electrolyte in high-temperature fuel cells or in oxygen sensors. From Fig. 2, we see that at low temperatures (e.g. 178 °C) arcs 2 and 3 appear while at high temperatures arcs 1 and 2 are obtained. Further we see that only arc 1, the electrode arc, has a strong dependence on partial pressure of oxygen of the ambient gas. These results show, however, that the behavior is more complex than that predicted from the schematic diagram of Fig. 1b. Firstly, the arcs are not full semi-circles but are somewhat depressed (as shown by the sloping lines drawn in Fig. 2). This result can be interpreted as meaning that each arc corresponds to a narrow distribution of R-C circuit elements rather than to single values. For simplicity we ignore this fact for the present. Secondly, it is found that the electrode contribution can involve more than a single arc. This will be discussed below. Nevertheless, the model of Fig. 1b can serve as the basis for extracting appropriate parameters. The two intersection points R_{12} and R_{23} are clearly related to the equivalent-circuit parameters by

$$R_{23} = R_{\ell} \tag{3}$$

and

$$R_{12} = R_{\ell} + R_{gb} \tag{4}$$

so that $R_{12} - R_{23}$ gives R_{gb}. Each of these resistances can be converted into a conductivity, σ, in the usual way by the relation

$$\sigma = d/AR \tag{5}$$

where d is the thickness and A the area of the sample. The results may then be plotted on a conductivity plot, log σT vs. $1/T$, as shown in Fig. 3. Here the lower curve (solid triangles) is obtained from R_{12} and the upper curve (open triangles) from R_{23}. In addition, results of four-probe d.c. measurements, which are plotted as open circles, show excellent agreement with R_{12}, thus firmly establishing that both arcs 2 and 3 are due to the

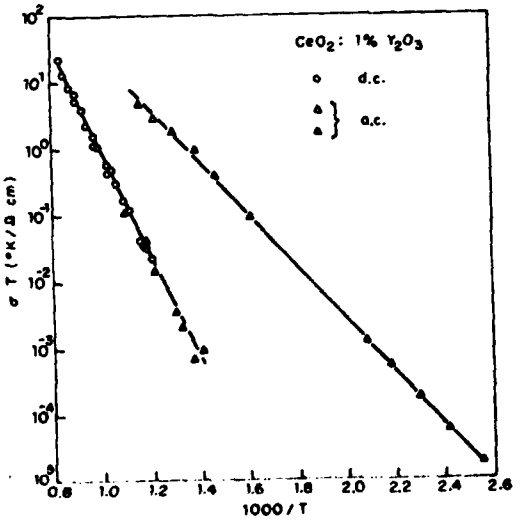

Fig. 3. Conductivity plots for a CeO_2:1% Y_2O_3 sample. Upper curve, obtained from the intersection R_{23} represents the lattice conductivity. Lower curve, consisting of a.c. measurements from R_{12} intersection, as well as d.c. 4-probe data, is dominated by the grain-boundary effect. From Ref. [9].

electrolyte. Both curves can be fitted to the conventional Arrhenius-type relation

$$\sigma T = B \exp(-H/kT) \qquad (6)$$

in which H is the activation enthalpy.

We have obtained useful information from each of the three arcs. From arc 3 we have obtained the lattice conductivity as a function of temperature, composition and dopant [9,10]. Considering that oxygen-ion vacancies are introduced as charge compensation for the dopant ions, one might expect a monotonically increasing conductivity as the dopant concentration increases. It is found instead that σ goes through a sharp maximum as a function of dopant concentration as shown for Y_2O_3 dopant in Fig. 4. At the same time, the activation enthalpy goes through a minimum. These results show that strong defect interactions suppress the conductivity beyond a concentration of 4-6 mole % dopant. The study of defect interactions in systems of high concentration is a subject of great interest and one which requires further study. Similarly, it was found that for different trivalent cation dopants of the same composition, the highest conductivity and lowest activation enthalpy H occur for a dopant whose size is closest to that of the host cation [10]. Such a result means that strain energy terms play an important role in determining H, a result that has recently been verified by computer simulation calculations [11]. From a practical viewpoint, these studies show how best to optimize the lattice conductivity with respect to dopant species and dopant concentration.

In most applications of solid electrolytes, one wishes to achieve the maximum possible overall d.c. conductivity. Accordingly the grain-boundary effect cannot be ignored. In fact, Fig. 3 shows that the overall conductivity can be as much as 100x lower than the lattice conductivity due to the grain-boundary effect. Similar effects are prevalent for other solid electrolytes, e.g. in β-alumina which is the electrolyte in the much publicized sodium-sulfur battery [12]. In the present case, particularly because $H_{gb} >> H_\ell$ (see Fig. 3), we can only interpret the electrical

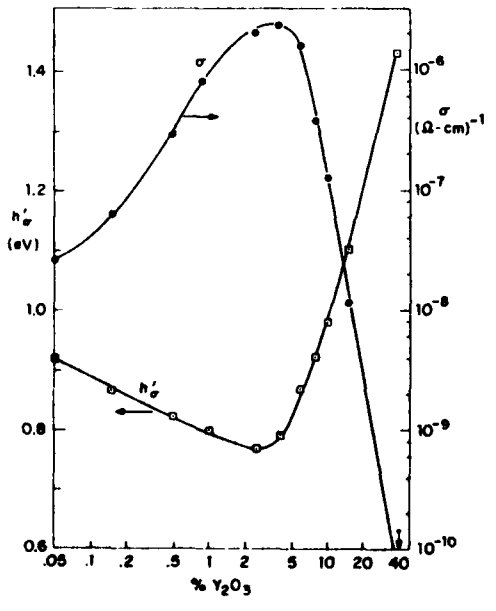

Fig. 4. Variation of conductivity σ (at 182 °C) and of activation enthalpy with composition, for CeO_2 - Y_2O_3 solid solutions. From Ref. [9].

effects in terms of the existence of a continuous (very poorly conducting) blocking layer, presumably associated with grain boundaries. In order to verify the presence of such a layer and to determine its origin, we examined thinned (ion-milled) samples by STEM (scanning transmission electron microscopy) in combination with microanalysis by EDAX (Energy Dispersive X-ray Microanalysis) and EELS (Electron Energy Loss Spectroscopy) [13]. A number of microstructural features were observed in this study, but the one most relevant seemed to be the presence of "thick boundaries", as shown in Fig. 5, i.e. layers of $\gtrsim$500A thickness which seem to be continuous. These were generally found to be an amorphous phase which had Si as its major cationic constituent. This silica-type phase did not surround each grain, however, but appeared around a small agglomerate of grains. In order to determine whether the presence of Si as an impurity is indeed responsible for the grain-boundary effect, we have very recently succeeded in preparing doped ceria samples from starting materials that were essentially silicon free. Our measurements show that in such a material the grain boundary effect is virtually eliminated.

The remaining arc (arc 1 in Figs. 1b and 2) is that due to electrode effects. Actually electrode processes are very complex and rarely give rise to just a single arc [14]. For the case of oxygen-ion conductors, we have carried out extensive studies with porous Pt-paste electrodes as well as a variety of others [15]. The simplest behavior (i.e., a single depressed arc) was observed for freshly prepared Pt-paste electrodes at relatively high oxygen partial pressures. With the aid of an auxiliary technique, called the current-interruption method [15], it was possible to show that, in this simplest case, the electrode process is controlled by a charge-transfer mechanism, in which an adsorbed oxygen adatom O_{ad} undergoes the reaction

$$O_{ad} + 2e^{-} + V_{o} = O^{=} + V_{ad}$$

where V_o and V_{ad} are lattice oxygen vacancy and vacant adsorbed site, respectively. The cathodic reaction goes from left to right and the anodic

Fig. 5. STEM microstructure of a sintered CeO_2:6% Gd_2O_3 sample showing "thick boundaries" of an amorphous silica phase. From Ref. [13].

in reverse. At low oxygen pressures or when the electrode has aged under high temperature or high current, an increase in Z" on the low-frequency side of the arc takes place. This is related to a transport limited process, or "concentration polarization."

DIELECTRIC AND ANELASTIC RELAXATION

Because of important similarities we will treat these two techniques together. In both cases an alternating field is used, electric and stress fields, respectively. We measure the fractional energy loss per cycle in the form of the quantity tan δ, where δ is the angle by which the response (polarization or strain, respectively) lags behind the applied field. In both cases the simplest behavior takes the form of the well-known Debye peak as a function of frequency:

$$\tan \delta = \Delta \cdot \omega\tau/(1 + \omega^2\tau^2) \tag{7}$$

where Δ is a measure of the strength of the relaxation process and τ is the relaxation time. In the case of dielectric or anelastic relaxations due to defect pairs (or higher clusters), Δ is proportional to the defect concentration and to the square of the electric or elastic dipole strength of the defect, respectively. On the other hand, the reciprocal τ^{-1} is related to the frequency of the controlling ionic migration process and is therefore thermally activated:

$$\tau^{-1} = \nu_0 \exp(-H_r/kT) \tag{8}$$

where H_r is the activation enthalpy for relaxation. Because of Eqs. (7) and (8), it is possible to observe tan δ either as a peak in frequency at constant temperature or a peak in temperature at constant frequency. For more complex processes, tan δ must be written as a summation over expressions of the type Eq.(7),and the corresponding peak is then broader than a simple Debye peak [16].

For dielectric relaxation an alternative to the a.c. tan δ measurement is available. It is called the TSDC (thermally stimulated depolarization current) method (also known as ITC) [17]. This method offers an extremely high sensitivity and therefore can detect the reorientation, under electric field, of electric dipoles at concentrations as low as 1 ppm. It has been applied to ceramics of the type already discussed [18], but for lack of space we will not be able to cover this work here.

To illustrate the use of these relaxation techniques we turn instead to a different problem, that of the frequency instability of quartz crystals. It is well known that α-quartz, due to its piezoelectric property, can be fabricated into resonators that vibrate at a fixed frequency. A common application is to control time pieces (i.e. watches). But applications of such resonators to controlling satellites and guidance systems demand far greater frequency stability, often to as much as 1 part in 10^9 or 10^{10}, even in radiation environments. Frequency instabilities under irradiation are found to be closely linked to impurities present in these crystals, one of the most important of which are alkali ions, e.g. Na^+ or Li^+ [19]. These alkalis are present in the crystal as compensation for the impurity Al^{3+}, which sits on Si^{4+} site and is deficient one positive charge. In recent years, techniques have been developed for replacing alkalis by H^+ or one alkali with another by a process of electrodiffusion or

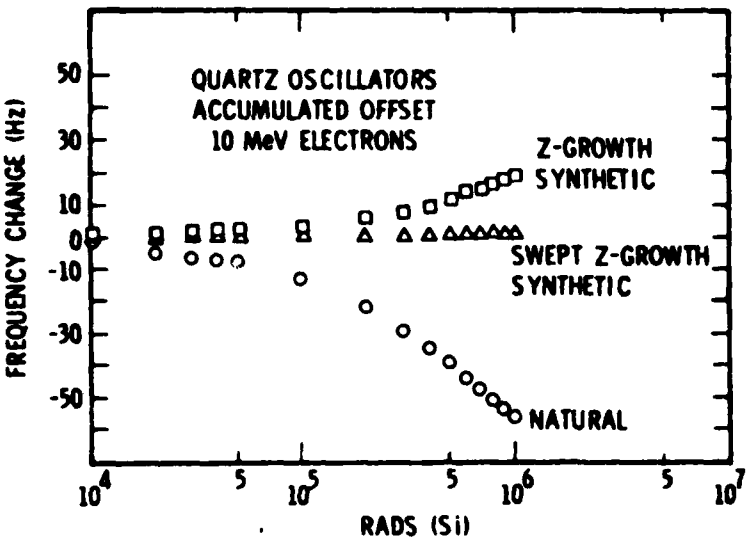

Fig. 6. Effect of electron irradiation on the room-temperature frequency change, δf, of 5 MHz quartz-crystal resonators. From Ref. [21].

"sweeping" [20]. In this process the crystal is treated at elevated temperature under a strong d.c. electric field in an appropriate environment. Also, methods of hydrothermal growth have made possible the production of synthetic quartz crystals that are often far lower in impurity content than natural crystals. Figure 6 shows the effect of electron irradiation at room temperature on three quartz crystals, a synthetic and a natural, both as grown, and on the same synthetic crystal after sweeping to replace alkali ions with H^+. The scale of frequency changes in this graph is very large compared to the best present-day requirements. Nevertheless, the figure shows that H^+ sweeping greatly reduces the frequency change that takes place under irradiation. Thus we see that alkalis contribute to δf.

One reason for a frequency offset at room temperature can be the occurrence of an anelastic relaxation peak at lower temperatures. The

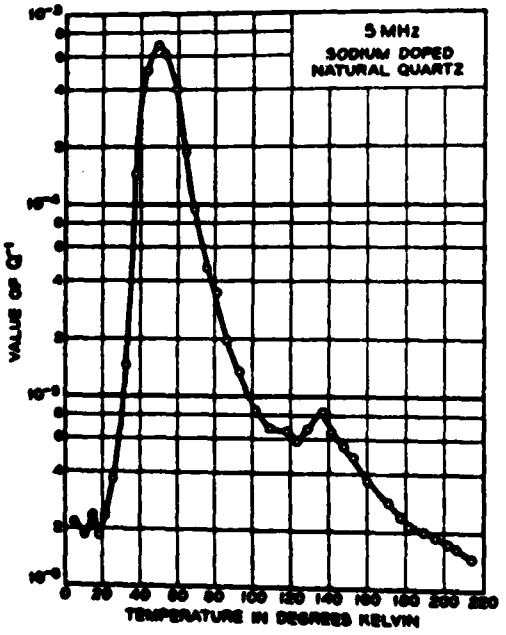

Fig. 7. Anelastic loss (internal friction, Q^{-1}) of a Na-doped quartz crystal as a function of temperature. From Ref. [20].

formal theory of anelasticity [16] shows that the presence of an anelastic peak given by Eq. (7) produces a frequency depression

$$\delta f/f = - \Delta/2 \qquad (9)$$

at all temperatures above the peak, where δf is the change in frequency relative to a defect-free crystal. In other words, to understand a frequency offset at room temperature requires that we know about relaxation peaks that occur below room temperature. Such peaks are indeed prevalent. For quartz crystals containing Na^+, a prominent pair of anelastic peaks is found at low temperatures, as shown in Fig. 7. A comparable pair of peaks is observed in dielectric relaxation [22]. These have low activation energies (H_r = 0.05 and 0.14 eV, respectively) and are attributed to the Na^+ being bound to a substitutional Al^{3+}, with the Na^+ residing in the interstitial channel. No such peaks due to Al-Li pairs have been found in spite of a careful search for them [23], presumably because the Li^+ sits on a 2-fold axis of symmetry. Irradiation produces important changes in these defects. Electron-hole pairs generated serve to free alkali ions from the Al^{3+} and to create Al-h (aluminum-hole) pairs instead. The migration of the alkali can be observed as conductivity enhancement immediately after irradiation [24]. It is not yet clear which defects serve as the traps at which the alkali ions terminate, but such trapping sites probably also capture one or more electrons. The Al-Na peaks are eliminated or reduced by the irradiation and, instead, new large peaks can be observed both by anelastic and dielectric loss measurements. Figure 8 shows such dielectric loss peaks for both Na^+- and Li^+- containing crystals. Similar anelastic peaks have been observed [25]. It is not yet clear as to whether these peaks are due to Al-h centers or to alkali centers which are created by the trapping of Li^+ or Na^+ freed by the irradiation. Nevertheless,

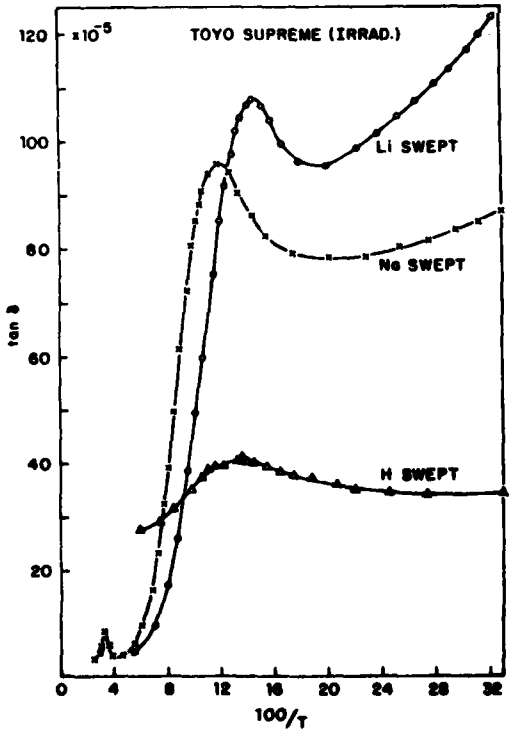

Fig. 8. Dielectric loss of Li-swept, Na-swept and H-swept synthetic quartz following room-temperature X-irradiation. From Ref. [24].

Eq. (9) shows that the elimination of a low-temperature anelastic relaxation peak by irradiation results in an increase in frequency, while the creation of a new peak results in a frequency decrease. Thus, it is clear that the solution to questions concerning frequency instabilities at room temperature lies in a better understanding of these low-temperature relaxation phenomena.

In conclusion, it was intended to show how the methods described herein give insight into ionic migration in ceramic materials. These methods can be usefully complemented by other widely used techniques such as diffusion and NMR measurements. Together, they give the type of insight into defect migration mechanisms that make it possible to eliminate practical problems or to determine conditions of maximum performance.

ACKNOWLEDGMENTS

The author wishes to acknowledge the contributions of his present and former associates: Drs. Da Yu Wang, H. Jain, J. Toulouse and R. Gerhardt-Anderson, and the support received from both the U.S. Department of Energy and the U.S. Air Force, RADC.

REFERENCES

1. S. Geller, ed., "Solid Electrolytes", Topics in Applied Physics vol. 21, Springer-Verlag, Berlin, 1977.

2. P. Hagenmuller and W. van Gool, eds., "Solid Electrolytes", Academic Press, New York, 1978.

3. E.C. Subbarao, ed., "Solid Electrolytes and Their Applications", Plenum Press, New York, 1980.

4. W. van Gool, ed., "Fast Ion Transport in Solids", North-Holland, Amsterdam, 1973.

5. G.D. Mahan and W.F. Roth, eds., "Superionic Conductors", Plenum Press, New York, 1976.

6. P. Vashishta, J.N. Mundy and G.K. Shenoy, eds., "Fast Ion Transport in Solids", North-Holland, Amsterdam, 1979.

7. J.B. Bates and G.C. Farrington, eds., "Fast Ionic Transport in Solids", North-Holland, Amsterdam, 1981.

8. Da Yu Wang and A.S. Nowick, J. Solid State Chem. 35 (1980) 325.

9. Da Yu Wang, D.S. Park, J. Griffith and A.S. Nowick, Solid State Ionics 2 (1981) 95.

10. R. Gerhardt-Anderson and A.S. Nowick, Solid State Ionics 5 (1981) 547.

11. V. Butler, C.R.A. Catlow, B.E.F. Fender and J.H. Harding, Solid State Ionics 8 (1983) 109.

12. R.W. Powers and S.P. Mitoff, J. Electrochem. Soc. 122 (1975) 226.

13. R. Gerhardt-Anderson, A.S. Nowick, M.E. Mochel and I. Dumler, Proc. Conf. High Temperature Solid Oxide Electrolytes, ed. F.J. Salzano, Brookhaven National Laboratory 1983, vol. 1, p. 225.

14. J.R. Macdonald, in "Electrode Processes in Solid State Ionics", M. Kleitz and J. Dupuy, eds., p. 149, Reidel Publ. Co., Dortrecht-Holland, 1976.

15. Da Yu Wang and A.S. Nowick, J. Electrochem. Soc. 126 (1979) 1155, 1166; 127 (1980) 113; 128 (1981) 55.

16. A.S. Nowick and B.S. Berry, "Anelastic Relaxation in Crystalline Solids", Academic Press, New York, 1972.

17. C. Bucci, R. Fieschi and G. Guidi, Phys. Rev. 148 (1966) 816.

18. Da Yu Wang and A.S. Nowick, J. Phys. Chem. Solids 44 (1983) 639.

19. J.C. King and H.H. Sander, Rad. Effects 26 (1975) 203.

20. D.B. Fraser, in "Physical Acoustics" vol. 5, W.P. Mason, ed., p. 59, Academic Press, New York, 1968.

21. B.R. Capone, A. Kahan, R.N. Brown and J.R. Buckmelter, IEEE Trans. on Nucl. Sci. NS-13 (1966) 130.

22. D.S. Park and A.S. Nowick, Phys. Stat. Sol. (a) 26 (1974) 617.

23. J. Toulouse, E.R. Green and A.S. Nowick, in "Proc. 37th Ann. Symp. on Frequency Control", 1983, p.125, U.S. Army ERADCOM.

24. H. Jain and A.S. Nowick, J. Appl. Phys. 53 (1982) 485.

25. J.J. Martin, L.E. Halliburton and R.B. Bossoli, in "Proc. 35th Ann. Symp. on Frequency Control", 1981, p. 317.

MISSION
of
Rome Air Development Center

RADC plans and executes research, development, test and selected acquisition programs in support of Command, Control Communications and Intelligence (C^3I) activities. Technical and engineering support within areas of technical competence is provided to ESD Program Offices (POs) and other ESD elements. The principal technical mission areas are communications, electromagnetic guidance and control, surveillance of ground and aerospace objects, intelligence data collection and handling, information system technology, solid state sciences, electromagnetics and electronic reliability, maintainability and compatibility.

Printed by
United States Air Force
Hanscom AFB, Mass. 01731

END

FILMED

DTIC